JOURNAL OF ADVANCES IN MODELING EARTH SYSTEMS, VOL. 5, 1–24, doi:10.1002/jame.20022, 2013

Representation of natural and anthropogenic land cover change in MPI-ESM

C. H. Reick,[1] T. Raddatz,[1] V. Brovkin,[1] and V. Gayler[1]

Received 27 July 2012; revised 8 February 2013; accepted 14 February 2013.

[1] The purpose of this paper is to give a rather comprehensive description of the models for natural and anthropogenically driven changes in biogeography as implemented in the land component JSBACH of the Max Planck Institute Earth system model (MPI-ESM). The model for natural land cover change (DYNVEG) features two types of competition: between the classes of grasses and woody types (trees, shrubs) controlled by disturbances (fire, windthrow) and within those vegetation classes between different plant functional types based on relative net primary productivity advantages. As part of this model, the distribution of land unhospitable to vegetation (hot and cold deserts) is determined dynamically from plant productivity under the prevailing climate conditions. The model for anthropogenic land cover change implements the land use transition approach by Hurtt et al. (2006). Our implementation is based on the assumption that historically pastures have been preferentially established on former grasslands (''pasture rule''). We demonstrate that due to the pasture rule, deforestation reduces global forest area between 1850 and 2005 by 15% less than without. Because of the pasture rule the land cover distribution depends on the full history of land use transitions. This has implications for the dynamics of natural land cover change because assumptions must be made on how agriculturalists react to a changing natural vegetation in their environment. A separate model representing this process has been developed so that natural and anthropogenic land cover change can be simulated consistently. Certain aspects of our model implementation are illustrated by selected results from the recent CMIP5 simulations.

Citation: Reick, C. H., T. Raddatz, V. Brovkin, and V. Gayler (2013), Representation of natural and anthropogenic land cover change in MPI-ESM, *J. Adv. Model. Earth Syst.*, *5*, doi:10.1002/jame.20022.

1. Introduction

[2] Climate can be easily recognized from the land cover, in particular from the vegetation cover. Therefore, it is no surprise that the first quantitative classification of world climates introduced by the plant physiologist *Koeppen* [1900] was based on land cover [see also *Sanderson*, 1999]. On the other hand, land cover is not only an indicator of climate but is also shaping the climate because the various exchange fluxes between land and atmosphere (energy, momentum, water, carbon, etc.) may be quite different for different types of land cover. From climate simulations we know that in a world with maximum vegetation cover, certain regions would be 8 K cooler than in a world with deserts everywhere [*Kleidon et al.*, 2000], and if the continents would be completely sealed against water evaporation, regionally temperatures would rise by more than 10 K [*Goessling and Reick*, 2011]. But it is not just that vegetation cover modifies climates, the coupling between vegetation and climate may even be so tight that the developing climate can only be understood by considering the combined dynamics of climate and vegetation. First indications for such a behavior were found by *Claussen* [1997, 1998] in early coupled climate-vegetation simulations. He found bistable solutions for vegetation cover and climate over North Africa. Today, feedbacks between vegetation and climate are generally considered an important element for understanding the Earth system [see e.g., *Kabat et al.*, 2004; *Chapin et al.*, 2008]. Accordingly, for realistic climate simulations not only a realistic land cover, but also a realistic land cover dynamics is needed.

[3] When performing climate simulations, one way to achieve a realistic land cover is to prescribe it from the observed land cover. But when studying climates that are very different from today, this approach fails. An early way to tackle this problem was to use so-called ''bioclimatic limits'' that determine the range in climate space where particular types of vegetation are able to exist [*Sykes et al.*, 1996; *Harrison et al.*, 2010]. By such

[1]Max Planck Institute for Meteorology, Hamburg, Germany.

1942-2466/13/10.1002/jame.20022

an approach, it is implicitly assumed that climate change is so slow that the vegetation distribution can easily follow changes in climate. But vegetation needs time to adapt: especially forests will stay even under unfavorable climate conditions for times of the order of the lifetime of individual trees (decades to centuries) [*Larcher*, 1994]. If climate change is significant at this time scale, the concept of bioclimatic limits will thus not be sufficient to simulate changes in vegetation distribution consistently with climate. Therefore, as part of third generation land surface models [*Pitman*, 2003], other more dynamical approaches have been developed accounting explicitly for internal time scales of vegetation. Such models are commonly called dynamic global vegetation model (DGVM). Whereas concepts for modeling the physical processes at the land-atmosphere interface are converging [*Pitman*, 2003], the approaches for modeling changes in biogeography dynamically are quite diverse and partially ad hoc [*Prentice et al*., 2007]. Although DGVMs have in common that fundamental ecological processes like establishment, mortality, competition, and partly also disturbances (e.g., wildfires) are explicitly incorporated, their representation in the models and thus the underlying dynamical equations are rather different. A comprehensive overview comparing the different approaches is still missing [see, however, *Cramer et al*., 2001; *McGuire et al*., 2001; *Sitch et al*., 2008; *Quillet et al*., 2010].

[4] Besides changes in natural vegetation, land cover is also modified by humans, in particular by the expansion of agriculture. Attempts to model also such processes dynamically are under way [*Lemmen et al*., 2011] but are quantitatively not sufficiently developed to be implemented into DGVMs. Accordingly, in climate and Earth system simulations anthropogenic land cover change needs to be prescribed. Most naturally, information on the location of agricultural areas is fed yearly into the model by a sequence of land cover maps. This has been done in numerous studies [see, e.g., *Brovkin et al*., 1999, 2006; *Pitman et al*., 2009; *Pongratz et al*., 2010].

[5] A realistic implementation of anthropogenic land cover change is especially important for deriving reliable estimates of CO_2 emissions from anthropogenic land cover change. For such studies it is not the yearly *net change* in land use that determines the emissions, but here all changes during a year contribute (*gross change*). Accordingly, prescribing the net year-to-year change may lead to an underestimation of emissions. Until now the size of this underestimation is unknown, but already a decade ago *Houghton* [2000] argued that it may not be negligible because the example of the United States shows that the difference between net and gross changes in cropland area may be on average as large as 35%. The more modern representation of anthropogenic land cover change by *Hurtt et al*. [2006] fully accounts for such gross changes. Here not maps, but transition matrices between different types of land cover are prescribed for every year. Thereby, it is possible to derive also carbon emissions caused by circular transitions between land cover types that otherwise leave the net land cover distribution unchanged.

[6] The purpose of the present paper is to provide an in-depth description how land cover change is modeled in the land component JSBACH [*Raddatz et al*., 2007] of the atmosphere model ECHAM6 [*Stevens et al*., 2013], being together part of the Max Planck Institute Earth system model (MPI-ESM) [*Giorgetta et al*., 2013]. Like other DGVMs, the dynamic vegetation component of JSBACH, called DYNVEG, inherits representations of the major ecological processes to describe natural changes in biogeography. Tree cover from simulations with DYNVEG has been presented by *Brovkin et al*. [2009]. The component for anthropogenic land use is based on the approach by *Hurtt et al*. [2006]. This component replaces the older one that used sequences of maps [*Jungclaus et al*., 2010; *Pongratz et al*., 2009]. A specific feature of the new implementation of anthropogenic land cover change is the assumption of a preferred establishment of pastures on former grasslands (''pasture rule''). This pasture rule is plausible insofar as grasslands can be used immediately for herding without extra work for chopping trees. Such a rule has been introduced by *Houghton* [1999] to derive continental scale carbon emissions from land use change for North America and China. It accounts for the fact that ''much of today's grazing land was formerly grasslands'' [*Ramankutty et al*., 2006]. But despite its plausibility, the character of the rule is hypothetical. Therefore, its consequences for global forest cover will be analyzed here in some detail. Whereas it is quite straightforward to implement agricultural expansion at given distribution of natural vegetation, the converse problem, i.e., climate-induced changes in the distribution of natural vegetation at given distribution of agricultural lands, is complicated by the pasture rule because this introduces a history dependence of the distribution of vegetation not only for agricultural lands but also for the distribution of natural forests and grasslands. Therefore, JSBACH contains also a separate model combining natural and anthropogenic land cover change. This new setup is the basis for most simulations performed with MPI-ESM in the context of the Coupled Model Intercomparison Project Phase 5 (CMIP5). Results from these simulations are accessible via the CMIP5 gateway http://cmip-pcmdi.llnl.gov/cmip5.

[7] This paper is not the place to evaluate the quality of the land cover distribution arising in climate simulations with MPI-ESM from the model components described here: in terms of forest cover and albedo such an evaluation is found in a companion paper by *Brovkin et al*. [2013] in the same issue. Instead, the intention of the present paper is to give a thorough description of the components describing land cover change in JSBACH along with explanations why they have been set up in this way. Nevertheless, this paper also contains some selected simulation results from the suite of CMIP5 simulations with MPI-ESM to illustrate certain aspects of this particular implementation of land cover change. For this purpose we use exclusively results from the low-resolution setup called MPI-ESM-LR (see *Giorgetta et al*. [2013] for details).

[8] Such simulation results are presented mostly in the last section of this paper. In the previous five

sections first basic elements of the land surface description of JSBACH are explained, followed by separate sections for each of the three submodels describing land cover change in JSBSACH, the DYNVEG component, the component for anthropogenic land cover change, and the component marrying these two types of land cover dynamics. This block of model descriptions closes with a separate section explaining the order of calculations necessary to update the land cover in JSBACH, a glance to Figure 4 depicting this sequence may be helpful even upon a first reading. In addition, for better orientation Tables 1 and 2 provide a list of abbreviations and symbols used throughout this paper.

2. Representation of Land Cover in JSBACH: Basic Concepts

[9] The basic land surface unit in JSBACH is a grid cell that has a predefined geographic location. Each grid cell is split into "tiles" to allow for the representation of subgrid scale heterogeneity. In this so-called "mixed" or "mosaic" approach [*Koster and Suarez*, 1992], the tiles are not specified by their location in a grid cell, but only by the fraction of the grid cell they cover. Each of these tiles is associated with one of several vegetation types, a so-called "plant functional type" (PFT). Conversely, considering a particular grid cell not every PFT represented in JSBACH must be linked with a tile of that grid cell: for example, to save computational time it may be useful to link tropical PFTs only with tiles of grid cells in the tropics, but not in the boreal zone. Formally, the PFT concept links the mosaic of tiles with the various land cover processes: each PFT is globally endowed with particular properties characterizing the various processes JSBACH is accounting for. Examples for such properties are the type of photosynthetic pathway (C3, C4), the type of phenology (e.g., deciduous and raingreen) but also PFT-specific albedo or surface roughness.

Table 1. Abbreviations and Acronyms Used in This Paper

Abbreviation	Meaning
C	Depending on context: croplands or carbon
C3, C4	Photosynthetic pathways
CMIP5	Coupled Model Intercomparison Project Phase 5
DGVM	Dynamic global vegetation model
DYNVEG	Dynamic vegetation component of JSBACH
ECHAM6	Atmospheric component of MPI-ESM
ESM	Earth system model
F	"F-lands," i.e., forests and shrublands
G	Grasslands
GDD	Growing degree days
JSBACH	Land component of MPI-ESM
LPJ	Lund-Potsdam-Jena DGVM
MPI-ESM	Max Planck Institute Earth system model
MPI-ESM-LR	Low-resolution version of MPI-ESM
MPI-OM	Ocean component of MPI-ESM
N	Land covered by natural vegetation (F plus G)
NPP	Net primary productivity
P	Pastures
PFT	Plant functional type
RCP	Representative concentration pathway

[10] One peculiarity of JSBACH is that one land cover type is not associated to a tile: regions unhospitable for growth of plants like rocky surfaces or deserts are determined by prescribing for each grid cell a fraction $veg_{\max}$ of the grid cell area that is hospitable to the growth of vegetation. Accordingly, $1-\mathrm{veg}_{\max}$ is the fraction of unhospitable land in a grid cell, and the area in a grid cell accessible for vegetation V is given by

$$V_{\mathrm{veg}} = A\,veg_{\max}, \tag{1}$$

where A is the total area of the grid cell (m^2). But JSBACH is not using *area* to characterize the extent of a particular vegetation type, instead the *fraction* of the area covered by vegetation is used (compare Figure 1). Denoting by v_i the area covered by the PFT associated with tile i in a grid cell (m^2), such fractions are most naturally introduced by

$$f_i = \frac{v_i}{A}, \quad i = 1, 2, \ldots, K, \tag{2}$$

where K is the number of tiles in a grid cell. Obviously, $V_{\mathrm{veg}} = \sum_{i=1}^{K} v_i$ so that

$$\sum_{i=1}^{K} f_i + (1 - veg_{\max}) = 1. \tag{3}$$

[11] Because of the implicit handling of bare land it is sometimes more convenient to describe land cover only with respect to that part of the grid cell where vegetation can grow. Associated cover fractions are introduced by

$$c_i = \frac{v_i}{V_{\mathrm{veg}}} = \frac{f_i}{veg_{\max}}, \quad i = 1, 2, \ldots, K, \tag{4}$$

and they sum up to 1:

$$\sum_{i=1}^{K} c_i = 1. \tag{5}$$

3. Natural Land Cover Change

[12] In interaction with climate and atmospheric CO_2 the worldwide distribution of vegetation and deserts may change. The dynamics of such changes are simulated in JSBACH by the DYNVEG component. This section describes the leading principles behind DYNVEG and its basic equations.

3.1. Leading Principles

[13] DYNVEG is based on a number of principles. Mostly, these principles are common to many DGVMs. Nevertheless, to make the assumptions underlying

Table 2. Notation Used Throughout This Paper[a]

Symbol	Meaning	Equation
A	Total grid cell area (m^2)	(1)
a	Calibration parameter for calculation of desert fraction	(12)
α	Exponent controlling competition between woody PFTs	(7)
$\alpha_0^{(w)}, \alpha_0^{(g)}$	Minimum fire disturbance rates for woody and grass PFTs	(10)
b	Calibration parameter for the steepness of the transition between desert and vegetation	(12)
$C_{G,i}^{\max}$	Maximum living biomass found in PFT i during a particular year	–
$C_{\mathrm{LGa},i}, C_{\mathrm{LWa},i}$	Carbon density of above ground litter in living (LGa) and wood (LWa) biomass of PFT i ($mol(C)\ m^{-2}$)	–
c_i	Fraction of V_{veg} covered by PFT i (actual vegetation)	(4)
c_i^{pot}	Fraction of V_{veg} covered by PFT i or land cover type i in the absence of agriculture ("potential" vegetation cover)	(14)
c_C, c_P	Fraction of V_{veg} covered with croplands (C) and pastures (P)	(15)
c_F, c_G	Fraction of V_{veg} covered with F-lands (F: forests, shrublands) and grasslands (G)	(19)
c_F^{inst}	"Target" fraction of V_{veg} for F-lands (F) that would appear if all historical land use change would happen in one instant	(66)
c_N	Fraction of V_{veg} covered with natural vegetation ($c_N = c_G + c_F$))	(19)
$D^{(w)}(), D^{(g)}()$	Rates for shrinkage of woody and grass cover by disturbances (yr^{-1})	(7), (8)
$D_{\mathrm{fire}}^{(w)}(), D_{\mathrm{fire}}^{(g)}()$	Rates for shrinkage of woody and grass cover by vegetation fires (yr^{-1})	(9)
D_{wind}	Rate for shrinkage of vegetation by windthrow (yr^{-1})	(9)
d	Number of days in a particular year (at 1 January $d = 1$)	(46)
$\Delta_{i\triangleright j}$	Annual fraction of V_{veg} converted from land cover type i to type j	(23)
$\delta_{i\triangleright j}$	Daily fraction of V_{veg} converted from land cover type i to type j	(45)
$f(y)$	For year y the grid cell fraction with substantial vegetation cover	(12)
f_i	Fraction of grid cell covered by PFT i	(2)
$\mathrm{GDD}_{\min}$	Minimum growing degree days (°C d)	–
$\mathrm{GDD}_{\mathrm{base}}$	Base temperature for computing growing degree days (°C)	–
$\mathcal{G}$	Index set for grass PFTs	(8)
g_i	Fraction of V_{veg} covered by ith grass PFT	(6)
g	$=\sum_{k\in\mathcal{G}} g_k$	(12)
$\vec{g}$	$=(g_1, g_2, \ldots, g_{N^{(g)}})$	(7)
$\gamma_i^{(w)}, \gamma_i^{(g)}$	Time constant for mortality of ith woody and grass PFT (years)	(7), (8)
h	Time-averaged relative air humidity as proxy for litter humidity	(10)
h_0	Threshold of h for the appearance of vegetation fires	(10)
K	Number of PFTs in a grid cell	(2)
κ	Calibration parameter for the rate of disturbance by windthrow ($d\ m^{-2}$)	(11)
L	Average above ground carbon density of litter ($mol(C)\ m^{-2}$)	(10)
L_0	Threshold of L for the appearance of vegetation fires ($mol(C)\ m^{-2}$)	(10)
$\mathrm{LAI}^{\max}$	Maximum leaf area index found in a particular year ($m^2(leaf)\ m^{-2}(ground)$)	(12)
$N^{(w)}, N^{(g)}$	Number of woody and grass PFTs	(6)
N_d	Number of days in the considered year	(45)
$\overline{\mathrm{NPP}}_i$	Long-term average of NPP of PFT i ($mol(C)\ m^{-2}\ s^{-1}$)	(7)
q	Threshold parameter (multiple of average wind speed) for the occurrence of windthrow	(11)
sla_i	Specific leaf area of PFT i	–
$T_{i\triangleright j}$	Element of annual transition matrix $\mathbf{T}$ describing land conversion from land cover type i to j	(15)
$T_{i\triangleright j}^{(d)}$	Element of daily transition matrix $\mathbf{T}$ describing land conversion from land cover type i to j	(48)
$t_{i\triangleright j}$	Element of daily transition matrix $\mathbf{t}$ describing land conversion from PFT i to j	(18)
$\mathrm{TC}_{\min}, \mathrm{TC}_{\max}$	Minimum and maximum temperature of coldest month (°C)	–
$\mathrm{TW}_{\max}$	Maximum temperature of warmest month (°C)	–
$\tau_i^{(w)}, \tau_i^{(g)}$	Time constant for establishment of ith woody and grass PFT (years)	(7), (8)
$\tau_{\mathrm{fire}}^{(w)}, \tau_{\mathrm{fire}}^{(g)}$	Characteristic repetition time for fire disturbances of woody types and grasses (years)	(10)
τ_{desert}	Time delay for the development of deserts (years)	(13)
$\theta()$	Heaviside step function	(7)
u	Fraction of V_{veg} currently uncolonized by vegetation	(6)
v	Wind speed ($m\ s^{-1}$)	(11)
$\overline{v}$	Average maximum wind speed used to scale windthrow rate ($m\ s^{-1}$)	(11)
V_{veg}	Grid cell area (m^2) accessible to vegetation	(1)
v_i	Grid cell area (m^2) covered by PFT i	(2)
$veg_{\max}$	Fraction of grid cell accessible to vegetation	(1)
$\mathcal{W}$	Index set for woody PFTs	(7)
w_i	Fraction of V_{veg} covered by ith woody PFT	(6)
$\vec{w}$	$=(w_1, w_2, \ldots, w_{N^{(w)}})$	(7)

[a]The last column refers to the equation of first appearance; an entry "–" means that the symbol appears only in the text.

DYNVEG more transparent, it seems worth to state these principles explicitly:

Increase/reduction of vegetation cover: When individual plants die because they come to age or because of other causes (fire, windthrow, diseases, pests), the space left by them can be taken by other plants. This is the cause for gap formation and subsequent plant successions in forests [*Begon et al.*, 1999]. For PFTs this

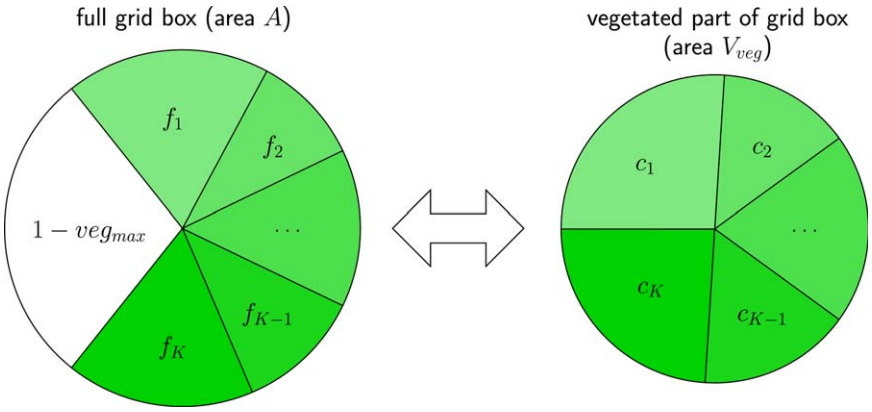

Figure 1. Tiling of grid cell and cover fractions: tile i has cover fractions f_i relative to the full grid cell and cover fraction c_i relative to the vegetated part of the grid cell.

means that their coverage is reduced by natural death or by disturbances (fires, windthrow) and increases by migration into spaces opened in this way. These open spaces are called in the following "uncolonized land," and the different vegetation types compete for this uncolonized land. There is a second type of increase/reduction of vegetation cover, namely, when regions unhospitable to vegetation expand or shrink (e.g., deserts). Changes in vegetation cover arising from this type of dynamics are assumed to affect all vegetation types equally, so that no competition is assumed here.

Competition by growth form: Part of the competitive advantages/disadvantages of woody vegetation as compared to grasses can be explained by their growth form: in the absence of disturbances trees and shrubs dominate because they take all the light by overgrowing the grasses at the bottom. Therefore, in DYNVEG woody and nonwoody PFTs are distinguished (see Table 3). On the other hand, because of the buildup of stems the growth of woody types is slow as compared to grasses so that after disturbances grasses can migrate faster into open spaces. Accordingly, grasses conquer uncolonized land first, and only later woody types appear. These structural advantages/disadvantages are represented in the model by (i) allowing grasses to access uncolonized land faster than woody types and (ii) by slowing down the expansion of grasses when uncolonized land gets rare, whereas the expansion rate of woody types is kept unaffected by the availability of uncolonized land: this slowing down assures that at low disturbance rates woody types dominate.

Table 3. PFTs Used in DYNVEG, Their Woodiness Type, and the Associated Time Constants Used in Equations (7) and (8)[a]

PFT	Type	$\tau_i = \gamma_i$ (years)
Tropical evergreen trees	Woody	30
Tropical deciduous trees	Woody	30
Extratropical evergreen trees	Woody	50
Extratropical deciduous trees	Woody	50
Raingreen shrubs	Woody	12
Deciduous shrubs	Woody	20
C3 grass	Nonwoody	1
C4 grass	Nonwoody	1

[a]For tree PFTs these time constants have been chosen such that a realistic tree cover is simulated (compare *Brovkin et al.* [2013]), and for the other PFTs the choice of time constants is guided by the idea that shrubs establish faster than trees, and grasses much faster than shrubs.

Competition by productivity: Net primary productivity (NPP) is the amount of carbon photosynthesized by plants that is available for growth and reproduction. Comparing the NPP of different vegetation types, a higher NPP can thus be considered to be an indicator for a competitive advantage if not other aspects like the growth form are dominating competition. Therefore, in DYNVEG, competition within the classes of woody and nonwoody types is modeled such that it is controlled by NPP: PFTs with higher NPP migrate into uncolonized land faster than PFTs with lower NPP. NPP is computed in JSBACH following the implementation of the Biosphere-Energy-Transfer-Hydrology (BETHY) model [*Knorr*, 2000], by first calculating gross primary productivity from solar radiation accounting for leaf area index, temperature, and soil water availability, and then subtracting autotrophic respiration calculated from maintenance and growth respiration.

Physiological constraints: To account for physiological constraints, PFTs are endowed with bioclimatic limits, i.e., climatic ranges in which a particular type of vegetation is able to exist. Such limits only prevent the *establishment* of vegetation, but once a vegetation has established and temperatures fall outside the range of bioclimatic limits, they do not prevent the further existence of the vegetation.

Unhospitable land: Vegetation can establish only when climate is such that at least in some years NPP is positive. This criterion determines the extent of cold and hot "deserts" or conversely, the amount of land available for vegetation.

Universal presence: It is assumed that every PFT is potentially present always and everywhere. This means that the dispersal of seeds is at the level of PFTs assumed to be much faster than all other processes relevant for their expansion ("seeds are everywhere").

3.2. Dynamics of Natural Vegetation Shifts

[14] The basic dynamical variables of DYNVEG are fractions of a unit area in a grid cell:

w_i: fraction of vegetated area covered by the ith woody PFT,

g_i: fraction of vegetated area covered by the ith nonwoody (i.e., grass) PFT, and

u: fraction of vegetated area currently without vegetation ("uncolonized land") because of fires or windthrow. These cover types make up the full grid cell:

$$u+\sum_{i=1}^{N^{(w)}} w_i+\sum_{i=1}^{N^{(g)}} g_i=1, \tag{6}$$

where $N^{(w)}$ and $N^{(g)}$ are the number of woody and grass PFTs, respectively, from Table 3. By this relation u can always be determined from w_i and g_i, so that only the latter are considered as independent variables. How u, w_i, and g_i are related to the JSBACH cover fractions introduced in the previous section will be described later.

[15] The dynamics of the cover fractions are governed by the coupled set of differential equations

$$\frac{\mathrm{d}w_i}{\mathrm{d}t}=\frac{\theta(u)w_i}{\tau_i^{(w)}}\frac{\overline{NPP}_i^{\alpha}}{\sum_{n\in\mathcal{W}} w_n\overline{NPP}_n^{\alpha}}-\frac{w_i}{\gamma_i^{(w)}}-w_iD^{(w)}(\vec{w},\vec{g}),\quad i\in\mathcal{W}=\{1,2,\ldots N^{(w)}\} \tag{7}$$

$$\frac{\mathrm{d}g_j}{\mathrm{d}t}=\frac{ug_j}{\tau_j^{(g)}}\frac{\overline{NPP}_j}{\sum_{n\in\mathcal{G}} g_n\overline{NPP}_n}-\frac{g_i}{\gamma_i^{(g)}}-g_jD^{(g)}(\vec{w},\vec{g}),\quad j\in\mathcal{G}=\{1,2,\ldots N^{(g)}\}. \tag{8}$$

These equations are integrated by iterating their Euler discretization at a daily time step (compare Figure 4). In both equations the first term on the right-hand side describes establishment, the second term describes reduction of vegetation cover by natural mortality, and the last terms represent reduction of vegetation cover by disturbances (fire, windthrow; see later). The establishment and natural mortality have their own characteristic time scales $\tau_i^{(w)}, \tau_i^{(g)}$, and $\gamma_i^{(w)}, \gamma_i^{(g)}$ for woody types and for grasses, although for lack of knowledge generally $\tau_i=\gamma_i$ has been chosen; the exact values are listed in Table 3. Mortality is assumed to be proportional to the abundance of the particular vegetation type. The function $\theta(u)$ is the step function, which is one for $u>0$ and otherwise zero.

[16] Establishment happens only on uncolonized land, i.e., in this model there is no immediate gain of area by a particular PFT at the cost of area covered by another PFT: in such a case the equations would contain explicit competition terms of the form w_iw_j, g_ig_j, or w_ig_j, as in the Top-down Representation of Interactive Foliage and Flora Including Dynamics (TRIFFID) model [*Cox*, 2001]. In DYNVEG competition between woody types and grasses arises only indirectly by their different dynamics with respect to uncolonized land: whereas grass establishes proportionally to the presence of uncolonized land (see the term ug_j in equation (8)), the establishment of woody types is assumed to be independent of the extent of uncolonized land, with the technically necessary exception that it is set to zero when all uncolonized land is already occupied (therefore, the step function in the term $\theta(u)w_i$ in equation (7)). Giving grasses a larger expansion rate than the woody types ($\tau_i^{(g)}\approx 1$ year, $\tau_i^{(w)}\approx$ several decades), this approach gives grasses a competitive advantage when large areas of uncolonized land are available, whereas woody types outcompete grasses when uncolonized land is rare. Since the availability of uncolonized land increases with the strength of disturbances (see later), DYNVEG implicitly assumes that the relative presence of grasses and woody types is controlled by the level of disturbance, in accordance with ecological theory [*Bond*, 2008].

[17] Considering the groups of woody and nonwoody types, the intragroup competition mechanism is different from the mechanism of intergroup competition: within a group the different PFTs compete by their long-term NPP average $\overline{NPP}_i$ (average over several years). This competition is implemented by weighting the expansion terms in equations (7) and (8) by the relative NPP of the particular PFT compared to total NPP within the particular vegetation group. When a PFT falls outside its bioclimatic limits (see section 3.4), its ability to expand is zero. Therefore, in this case the respective value of $\overline{NPP}_i$ is set to zero. The exponent α is an additional control parameter by which competition within the class of woody PFTs is further controlled. For $\alpha>1$ PFTs with high NPP are given an additional migratory advantage. Accordingly, α controls the time scale of succession, which is for tree species of the order of centuries [*Begon et al.*, 1999]. For typical relative differences in $\overline{NPP}_i$ this is assured by choosing $\alpha=1.5$.

[18] Finally, there are terms describing disturbance losses by wildfires and windthrow. These are described in the following section.

3.3. Disturbances

[19] DYNVEG accounts for two types of disturbances: vegetation fires and windthrow. These processes determine the disturbance rates $D(\vec{w},\vec{g})$ in equations (7) and (8) (yr^{-1}) which accordingly consist of separate contributions from fires and windthrow:

$$D^{(i)}(\vec{w},\vec{g})=D_{\mathrm{fire}}^{(i)}(\vec{w},\vec{g})+D_{\mathrm{wind}},\quad \text{for } i=w,g. \tag{9}$$

Note that the windthrow rate is independent of the cover fractions and set to zero for grasses because of negligible aerodynamic resistance.

[20] It is assumed that wildfires happen only if (i) sufficient above ground plant litter L is available for combustion (L must be larger than a threshold value L_0 chosen as $L_0=16.67$ mol(C) m^{-2}), and if (ii) the litter is sufficiently dry to catch fire. Such a relationship between humidity of plant litter and flammability is well supported by observations [*Catchpole et al.*, 2001].

Here, litter dryness is measured by a several weeks' average of relative air humidity (denoted by $\overline{h}$) of the lowest atmospheric level, and "sufficiently dry" then means that h must be lower than a certain threshold humidity h_0 (chosen as $h_0=70\%$). From experiments in grasslands it is known that once ignited, the spread of wildfires increases with decreasing fuel moisture, but the spread in the observational data is large [*Cheney et al.*, 1998]. Under these conditions the fire disturbance rate is assumed to increase linearly with decreasing humidity:

$$D^{(i)}_{\text{fire}}(\vec{w},\vec{g}) = \alpha_0^{(i)} + \frac{1}{\tau^{(i)}_{\text{fire}}} \begin{cases} \dfrac{h_0-\overline{h}}{h_0} & \text{if } L > L_0 \text{ and } \overline{h} < h_0, \\ 0 \quad \text{otherwise}, \end{cases}$$
$$\text{for } i=w,g. \tag{10}$$

Here $\alpha_0^{(w)}$ and $\alpha_0^{(g)}$ are minimum fire disturbance rates for woody types and grasses, and $\tau^{(w)}_{\text{fire}}, \tau^{(g)}_{\text{fire}}$ are the inverse of a characteristic frequency for the appearance of wildfires in woody types and grasses (with $\tau^{(w)}_{\text{fire}} > \tau^{(g)}_{\text{fire}}$ so that the fire rate for woody types is smaller than for grasses). This fire disturbance rate depends on the extent of woody types $\vec{w}=(w_1, w_2, \ldots)$ and grasses $\vec{g}=(g_1, g_2, \ldots)$ only via the value of the above ground litter L. Here DYNVEG is closely linked to the land carbon cycle in JSBACH that will be presented elsewhere. More precisely, L is the average above ground carbon litter density in the vegetated part of a grid cell. In JSBACH it is obtained from the cover fractions c_i (that are directly related to $\vec{w}$ and $\vec{g}$; see section 3.6) and above ground carbon litter densities in the so-called green litter carbon pool $C_{\text{LGa},i}$ (litter from nonlignified biomass) and the woody litter carbon pool $C_{\text{LWa},i}$ (litter from lignified biomass) by $L=\sum_i c_i\left(C_{\text{LGa},i}+C_{\text{LWa},i}\right)$ where the sum extends over all tiles in a grid cell.

[21] The disturbance rate for windthrow, which is only relevant to woody types, is modeled as

$$D_{wind} = \begin{cases} \kappa \dfrac{v}{\overline{v}} v^2 & \text{if } v > q\overline{v} \\ 0 & \text{otherwise} \end{cases}. \tag{11}$$

Windthrow is zero when the wind speed v is below a certain multiple q of the typical long-term average maximum wind speed $\overline{v}$. Using such an average wind speed as reference instead of a fixed prescribed wind speed accounts for adaptation of the local vegetation to the prevailing wind forces. The variable κ is a calibration parameter. If windthrow happens, the disturbance rate is set proportional to the acting wind power, which raises with the third power of the wind speed. On the other hand, because it is assumed that existing vegetation is adapted to the prevailing typical wind speeds, the formula is written in such a way that the disturbance rate is as well proportional to $v/\overline{v}$. The average maximum wind speed $\overline{v}$ is computed as a running mean over a period of several years. The variables q and κ are chosen such that windthrow leads to only a few severe storm damages per year in regions with high wind speeds (mainly extratropics). Since wind speed extremes depend on the resolution of atmospheric fields, κ and q must be chosen differently for different grid resolutions. For standard resolution of the CMIP5 simulations with MPI-ESM, $\kappa=0.01/365$ days/m^2 and $q=2.25$ have been chosen. Note that disturbances are computed at a daily time step.

[22] Whereas the losses in vegetation cover by windthrow are mutually independent between grasses and woody types, the disturbances by wildfires introduce an additional coupling: besides a small climate independent vegetation loss by fires (the terms $\alpha_0^{(w)}$ and $\alpha_0^{(g)}$ in equation (10)), the disturbance rates contain another component that is nonzero only if together the litter of grasses and woody types exceeds a particular threshold. Because of the threshold behavior and because litter production depends on the extent of grasses and woody types, this interaction induced by wildfires is nonlinear.

3.4. Bioclimatic Limits

[23] The global distribution of vegetation is determined not only by competition but also by climate-related physiological constraints: it may be too cold or too hot for a particular vegetation type to survive. Although the dynamics of DYNVEG are formulated independently of the particular set of PFTs chosen (except that it needs both, woody and grass PFTs), the formulation of these constraints depends heavily on the set of PFTs chosen. In our recent CMIP5 simulations we used the PFTs listed in Table 3, but this choice is by no means unique. In DYNVEG these climatic constraints are accounted for by setting the establishment term in equations (7) and (8) to zero if one of the limits listed in Table 4 is not fulfilled. Most of these values are

Table 4. Bioclimatic Limits Used in DYNVEG for Different Vegetation Groups[a]

	Tropical Trees		Extratropical Trees		Shrubs		Grasses	
	Evergreen	Deciduous	Evergreen	Deciduous	Raingreen	Deciduous	C3	C4
TC_{min}	15.5	15.5	−32.5	–	2.0	–	–	10.0
TC_{max}	–	–	18.5	18.5	–	−2.0	15.0	–
TW_{max}	–	–	–	–	–	18.0	–	–
GDD_{min}	–	–	350	350	900	300	–	–
GDD_{base}	5	5	5	5	5	5	5	5

[a]An entry "–" means that no limit is applied. TC_{min}: minimum temperature of coldest month (°C); TC_{max}: maximum temperature of coldest month (°C); TW_{max} maximum temperature of warmest month (°C); GDD_{min}: minimum growing degree days (°C d); GDD_{base}: base temperature for computing growing degree days (°C).

taken from the LPJ (Lund-Potsdam-Jena DGVM) [*Sitch et al.*, 2003], which can partly be justified by observations [*Sykes et al.*, 1996; *Harrison et al.*, 2010]. But whereas DYNVEG uses only two PFTs for extratropical trees, LPJ distinguishes here between needle-leaved and broad-leaved forests as well as temperate and boreal forests. Accordingly, in DYNVEG the bioclimatic ranges of extratropical forests had to be chosen wider than in LPJ: they were chosen such that they cover the full bioclimatic range of the extratropical forest types of LPJ. Thereby, in contrast to LPJ, in DYNVEG all extratropical forests are except for TC_{min} (see Table 4) subject to the same bioclimatic limits so that the geographic pattern of evergreen and deciduous forests is mostly determined by competition and not by numerous bioclimatic limits.

[24] Shrubs represent marginal vegetation, restricted in growth either by very dry and hot or by very cold conditions. Accordingly, the bioclimatic limits of rain-green shrubs are chosen to exclude them from areas with a cold winter and frequent frost, so that they appear only in dry tropical and subtropical regions. In contrast, deciduous shrubs, representing woody tundra, are excluded by bioclimatic limits from regions with a warm climate.

[25] The geography of the bioclimatic limits may shift in a simulation with a change in climate. Therefore, at the beginning of each simulated year it is analyzed whether bioclimatic limits are still met by the different PFTs. This is checked by comparing the limits with the respective climate variables. But before comparison, these climate variables are time-averaged to smooth out short-term climate variations by using an exponentially decreasing memory (e-folding time 20 years) that allows gradual adaptation to the actual climate. This is done for all limits based on the monthly averaged temperature, namely, TC_{min}, TC_{max}, and TW_{max} (compare Table 4). In contrast, for GDD_{min} just the previous year's value is used.

3.5. Dynamics of Unhospitable Land

[26] DYNVEG includes a small model to determine the extent of land unhospitable to vegetation, which can be cool deserts like in the arctic or hot deserts like the Sahara. The extent of unhospitable land determines the fraction of a grid cell veg_{max} where vegetation can grow (compare section 2) and is therefore another central element determining land cover in JSBACH.

[27] The model for unhospitable land is based on the idea that deserts develop when NPP gets too low so that vegetation is repeatedly not able to grow an extended canopy at least once during a year. Conversely, vegetation can grow where such an extended canopy can be developed. The fraction of a grid cell with substantial vegetation cover at least once in year y is estimated as

$$f(y)=\sum_{i\in\mathcal{W}} w_i\left(1-e^{-a\left(\mathrm{LAI}_i^{\max}\right)^b}\right) + \sum_{i\in\mathcal{G}} g_i\frac{g+u}{g}\left(1-e^{-a\left(\mathrm{LAI}_i^{\max}\right)^b}\right), \tag{12}$$

where $g=\sum_{k\in\mathcal{G}} g_k$ is the total grass fraction of vegetation, and $\mathrm{LAI}_i^{\max}$ is the maximum leaf area index that appeared during year y. In JSBACH it is determined from the maximum biomass in leaves by $\mathrm{LAI}_i^{\max}(y)=\mathrm{sla}_i C_{G,i}^{max}/3$, where $C_{G,i}^{max}$ is the maximum living biomass found in PFT i in the considered year. Here the biomass in leaves is assumed to be one third of the whole biomass because it includes also root and sapwood biomass (JSBACH is not distinguishing these plant parts in terms of carbon), and sla_i is the so-called specific leaf area relating the carbon content of leaves to their area. The parameter $a=1.95$ is chosen such that the simulated distribution of cold and hot deserts matches observations. It may be noted that with this choice of a for $\mathrm{LAI}_i^{\max}=1$ the expression $1-\exp(-a)$ gives a vegetation cover of approximately 85% which is still substantial. For woody types this cover is weighted in equation (12) by their cover fraction directly, whereas for grass types the extent of unhospitable land is included in the weighting because this is land that gets only temporarily available to vegetation by disturbances. The parameter $b=2$ describes the steepness of the transition between vegetation and desert and has been chosen to give a realistic distribution of deserts. Since one year of low vegetation growth does not make a desert, a delayed development is assumed: for the year y we calculate veg_{max} by

$$veg_{max}=\sum_{y'=-\infty}^{y} f(y')e^{-\frac{y-y'}{\tau_{\mathrm{desert}}}}, \tag{13}$$

where the time scale for development of unhospitable conditions is chosen as $\tau_{\mathrm{desert}}=50$ years.

3.6. Potential Natural Vegetation Cover

[28] In this section it is described how the DYNVEG cover fractions w_i, g_i, and u are translated into the JSBACH cover fractions c_i and veg_{max} introduced in section 2. Following the definition of *Westhoff and van der Maarel* [1973], the term "potential vegetation" denotes the distribution of vegetation that one would see under the ruling climate conditions in a world without humans. This is exactly what can be obtained from DGVMs in general [*Bond*, 2008], and DYNVEG in particular: a map of potential natural vegetation, which in the absence of anthropogenic land cover change is also the actual land cover. How the DYNVEG cover fractions relate to the actual cover fractions in the presence of anthropogenic land cover change is described in another section later.

[29] As indicated in the above list of basic principles, it is assumed that the competitive advantage of grasses compared to woody types is their expansion speed. This principle is used here to derive potential natural vegetation cover from the DYNVEG cover fractions, by assuming that only grass types expand within 1 year into areas formerly disturbed by vegetation fires or windthrow. Hence, in terms of JSBACH cover fractions, the fraction u of disturbed area is fully counted as

grasslands. Moreover, it is assumed that all grass types existing in the considered grid cell expand proportionally to their presence. Combining these considerations with equations (6) and (5) gives when accounting for (4),

$$c_i^{\mathrm{pot}} = \frac{1}{veg_{max}} \begin{cases} g_i \left(1 + \frac{u}{\sum_{j \in \mathcal{G}} g_j} \right) & \text{for } i \in \mathcal{G} \\ w_i & \text{for } i \in \mathcal{W}, \end{cases} \tag{14}$$

where $\mathcal{W}$ denotes the woody types, and $\mathcal{G}$ denotes the nonwoody types (grasses), and $veg_{\max}$ is given by (13). In the absence of land use, c_i^{pot} is the actual land cover c_i. To arrive at the land cover including land use, additional calculations are necessary (compare Figure 4). These will be presented in the following sections.

4. Anthropogenic Land Cover Change

[30] In JSBACH the model for anthropogenic land cover change is based on the *New Hampshire Harmonized Land Use Protocol*, for short called ''Harmonized Protocol'' in the following, which was developed by *Hurtt et al*. [2011] in preparation of the recent communitywide CMIP5 simulations to have a common data format for land use change for the new *representative concentration pathways* (RCPs), which are the new climate scenarios used in CMIP5 [*van Vuuren et al*., 2011a]. The Harmonized Protocol uses as input a sequence of so-called land use transitions [*Hurtt et al*., 2006]. The difference to the classic procedure prescribing the geographic land cover distribution and its development directly by a sequence of maps gets most obvious when considering a situation where the land cover transitions are such that before and after the land use transition the area of all PFTs is identical. Considering a particular grid cell, an example could be the simultaneous conversion of forests into pasture, pasture to croplands, and croplands to forest in that grid cell. Despite constant net area of the PFTs, such a cyclic conversion produces relocation of carbon between different carbon reservoirs and CO_2 emissions from land use change. Accordingly, the two approaches differ in the biogeochemical consequences of anthropogenic land use change. Nevertheless, the focus in the present paper is only on the representation of land cover change, the carbon aspects will be presented elsewhere (C. H. Reick et al., unpublished).

[31] The Harmonized Protocol is not based on PFTs but uses a classification characterizing vegetation cover only with respect to land use: two classes for natural vegetation (*primary* and *secondary*), and two classes of agricultural land cover: *crops* and *pastures*. By the difference between primary and secondary natural vegetation the Harmonized Protocol provides information on land use of natural vegetation: whereas lands with secondary natural vegetation show traces of current or past land use (e.g., in the form of wood harvest), primary natural vegetation has never been touched by man. But in order to make use of this information one had to implement models representing the land use of natural vegetation (e.g., in the form of forestry). Since such models have not been developed for JSBACH, in the implementation of the Harmonized Protocol the two classes of primary and secondary vegetation are lumped together into one large class of *natural* vegetation. This is done in a preprocessing step so that the actual data used from the (reduced) Harmonized Protocol to drive JSBACH contain only transitions between natural vegetation (N), crops (C), and pasture (P). Since JSBACH has no special representation of urban land cover, the additional transition data to/from urban land provided by the Harmonized Protocol are not used.

[32] The major challenge in implementing the Harmonized Protocol is to derive from its very coarse information on land use transitions between its broad land cover classes the much more detailed information on land use transitions between PFTs. To achieve this higher degree of detail, additional rules are needed. The selection of such rules is left to the modeler using the Harmonized Protocol. One such rule used in the JSBACH implementation of the Harmonized Protocol refers to the establishment of pastures: it is plausible that historically, if available, preferentially natural grasslands have been used for the grazing of sheep or cattle before laboriously clearing forests for this purpose. This priorization of grasslands will be one of several rules used in the following to obtain PFT transitions from the Harmonized Protocol. The full set of *land distribution rules* to derive the PFT transitions is:

(1) *Pasture rule*: Pastures expand first into grasslands before other natural vegetation is touched. For croplands there is no such priority. On abandonment of agricultural lands these rules are reversed.

(2) *Pathway rule*: This rule concerns the relative extent of plants with C3 and C4 photosynthetic pathways: in view of the lack of suitable data, on conversions the ratio between C3 and C4 types is kept fixed among grasslands, among crops, as well as among pastures.

(3) *Rule of equal relative gains and losses*: After accounting for the two rules above, following the expansion of crops and pastures all natural PFTs undergo the same relative loss. Similarly, on back conversion of agricultural lands to natural, the relative gain of natural PFTs with respect to the area maximally available for their extension is equal for all PFTs.

[33] Observational evidence for the pasture rule will be discussed in section 4.5. The rationale for this rule comes from the higher effort necessary to chop down trees to gain agricultural lands than making use of grasslands: the pasture rule plays only a role in mixed tree/grass environments because only there farmers have a choice. In such mixed environments forest sites have typically richer soils so that they are more suitable for crop growth; this may justify the effort of deforestation. In contrast, for grazing of livestock the advantage of a higher productivity at forest sites is marginal, so that it is easier to use grass sites directly. This latter remark explains at least partly also the pathway rule:

most probably the effort for conversion between pastures and grasslands is kept low so that grasses are left in place without sowing new grass types. For crops the situation may be different, but in the absence of additional information for another distribution of gains and losses this rule is still a pragmatic choice. The same holds true for the rule of equal relative gains and losses: because information on a possible preferential selection of one PFT over another during land conversion is missing, there is not much alternative to this rule.

4.1. Mathematical Formulation of the Problem

[34] Let **T** denote the (reduced) transition matrix of the Harmonized Protocol, i.e., an element $T_{i\triangleright j}$ denotes the fraction of area of land cover class i converted within 1 year to land cover class j; the land cover classes i and j used here are natural land (N), crops (C), and pastures (P). Originally, the Harmonized Protocol refers to fractions of area in a grid cell, but since box area and vegetated area are linearly related (see equation (4)), the transition matrix can as well be applied directly to the fractions of vegetated area. This is how the transition matrix is used in the following. Nevertheless, it should be noted that thereby it is implicitly assumed that upon expansion/shrinkage of vegetation cover, i.e., upon changes of $veg_{\max}$, areas converted upon land use change are larger/smaller than originally prescribed by the Harmonized Protocol. Since *Hurtt et al.* [2011] have ignored climate-induced changes in potential vegetation when deriving their transitions (they use fixed climate data for 1987–1988), generally an inconsistency between the Harmonized Protocol and Earth system simulations cannot be avoided. From this point of view, our approach is as reasonable as assuming that climate change has no influence on the transitions. One can argue that it is even more realistic, since human activities are closely related to the availability of natural resources.

[35] Let c_N, c_C, and c_P denote the fractions of the vegetated part of a grid cell covered by vegetation from classes N, C, and P. Then, the (reduced) Harmonized Protocol describes the annual transition in land cover by

$$\begin{pmatrix} c'_N \\ c'_C \\ c'_P \end{pmatrix} = \begin{pmatrix} T_{N\triangleright N} & T_{C\triangleright N} & T_{P\triangleright N} \\ T_{N\triangleright C} & T_{C\triangleright C} & T_{P\triangleright C} \\ T_{N\triangleright P} & T_{C\triangleright P} & T_{P\triangleright P} \end{pmatrix} \begin{pmatrix} c_N \\ c_C \\ c_P \end{pmatrix}, \qquad (15)$$

where $0 \le T_{i\triangleright j} \le 1$. Since N, C, and P make up the whole vegetation in a grid cell the land use transitions only repartition the vegetated part of the grid cell into these three cover types, leaving the total extent of vegetation in the grid cell unchanged so that

$$c'_N + c'_C + c'_P = c_N + c_C + c_P. \qquad (16)$$

Hence, because thereby independently of the values of the c_i one has $\sum_k c'_k = \sum_i c_i$, it follows from $\sum_k c'_k = \sum_k \sum_i T_{i\triangleright k} c_i = \sum_i c_i \sum_k T_{i\triangleright k}$ that

$$\sum_{k\in\{N,C,P\}} T_{i\triangleright k} = 1 \quad \text{for} \quad i \in \{N, C, P\}, \qquad (17)$$

i.e., the land of a particular class i can be distributed only once. Note that the diagonal elements $T_{i\triangleright i}$ denote that fraction of a class that remains unconverted.

[36] Actually, the above noted restriction $T_{i\triangleright j} \le 1$ is not immediately obvious: large areas of the world have in history undergone multiple cycles of deforestation and subsequent abandonment. Formally, this whole complicated process of deforestation and afforestation may together be considered a single land use transition. In such a combined transition, the total land cover fraction $\Delta_{P\triangleright N} = T_{P\triangleright N} c_P$ retransferred from pasture to natural may be much larger than c_P because $\Delta_{P\triangleright N}$ could include the same part of land that was repeatedly afforested after forest was transformed into pasture. Here, obviously, the time step of the land use protocol is of importance: it is plausible that within a year farmers do not deforest land for growing crops and afforest the same land in the same year. Hence, a time step of one year, as used in the Harmonized Protocol, is consistent with the assumption $T_{i\triangleright j} \le 1$. And this is also reflected in the data as provided by the New Hampshire group.

[37] The obvious aim is to translate equation (15) into an analogous equation for PFTs. The associated transition matrix will be called **t**, and its elements $t_{i\triangleright j}$ denote the fraction of area of PFT i converted within one year to PFT j. Because of the tiling of grid cells in JSBACH (see section 2), the set of PFTs allowed in a grid cell is restricted to a subset of all possible PFTs. Therefore in the equation analogous to equation (15) not all PFTs, but only those allowed in a grid cell have to show up. Hence, calling c_i the fraction of a grid cell covered by the ith PFT in a grid cell the aim is to translate equation (15) into

$$\begin{pmatrix} c'_1 \\ c'_2 \\ \vdots \\ c'_K \end{pmatrix} = \begin{pmatrix} t_{1\triangleright 1} & t_{2\triangleright 1} & \cdots & t_{K\triangleright 1} \\ t_{1\triangleright 2} & t_{2\triangleright 2} & \cdots & t_{K\triangleright 2} \\ \vdots & \vdots & \ddots & \vdots \\ t_{1\triangleright K} & t_{2\triangleright K} & \cdots & t_{K\triangleright K} \end{pmatrix} \begin{pmatrix} c_1 \\ c_2 \\ \vdots \\ c_K \end{pmatrix}, \qquad (18)$$

where K is the number of PFTs in the particular grid cell considered. Obviously, equations analogous to equations (16) and (17) hold for PFT-related cover fractions and elements of the transition matrix **t**.

[38] To obtain the transition matrix **t** from the transition matrix **T** according to the above mentioned rules, a complicated extremization problem has to be solved: according to the pasture rule the transitions from pastures to grasslands have to be maximized, and the back transitions minimized. Here natural vegetation is implicitly divided into grasslands and other natural vegetation; these types of vegetation cover will be abbreviated by "G" and "F," respectively, in the following, where "F" stands for "forest" well knowing that natural nongrassland vegetation can also be different from forests, like bushlands or tundra. With this notation the associated cover fractions obey

$$c_N = c_G + c_F. \qquad (19)$$

[39] It turns out to be convenient to solve first a reduced transition problem between the cover classes G, F, P, and C, before continuing with the full problem for all PFTs. Accordingly, first the (extended) 4 × 4 transition matrix **T** describing the dynamics between these four land cover classes has to be determined:

$$\begin{pmatrix} c'_G \\ c'_F \\ c'_C \\ c'_P \end{pmatrix} = \begin{pmatrix} T_{G\triangleright G} & T_{F\triangleright G} & T_{C\triangleright G} & T_{P\triangleright G} \\ T_{G\triangleright F} & T_{F\triangleright F} & T_{C\triangleright F} & T_{P\triangleright F} \\ T_{G\triangleright C} & T_{F\triangleright C} & T_{C\triangleright C} & T_{P\triangleright C} \\ T_{G\triangleright P} & T_{F\triangleright P} & T_{C\triangleright P} & T_{P\triangleright P} \end{pmatrix} \begin{pmatrix} c_G \\ c_F \\ c_C \\ c_P \end{pmatrix}. \tag{20}$$

Because the four elements of the lower right 2 × 2 submatrix do not involve transitions to or from F or G they are identical to the respective entries in equation (15) and are thus directly known from the (reduced) Harmonized Protocol. Moreover,

$$T_{F\triangleright G} = T_{G\triangleright F} = 0 \tag{21}$$

because in our implementation on land use change humans do not induce direct transitions between natural land cover classes. (This is actually different from the original Harmonized Protocol, where transitions from primary to secondary vegetation are induced by harvest. This harvest is treated in JSBACH independently.) The other matrix elements are unknowns of the problem, as well as the cover fractions c_G, c_F, c'_G, c'_F, although of these the first two are related by equation (19) and the second two obey analogously

$$c'_N = c'_G + c'_F. \tag{22}$$

[40] Please note that here and in the following the same symbol **T** is used for the (reduced) 3 × 3 and the (extended) 4 × 4 transition matrix, because several elements are identical and the meaning is always recognizable from the context.

4.2. Application of the Pasture Rule

[41] In this section the 4 × 4 matrix for the extended land use transitions equation (20) is derived from the 3 × 3 matrix for the reduced land use transitions (15) by applying the pasture rule. In the following the term "F-lands" is used for land cover of type "F."

[42] Technically, the pasture rule means that *Agricultural expansions* proceed in the following order of conversions:

(1) $G \rightarrow P$: For pastures first grasslands are used.
(2) $F \rightarrow P$: Only if grasslands are exhausted, pastures are established on F-lands.
(3) $G+F \rightarrow C$: For croplands the remaining grasslands and F-lands are used at equal proportion.

Shrinkage of agricultural lands is for simplicity chosen to proceed in reverse order:

(1) $C \rightarrow F+G$: First croplands are given back to natural grasslands and F-lands according to their relative availability.
(2) $P \rightarrow F$: Next, pastures are given back to F-lands.
(3) $P \rightarrow G$: Finally, if F-lands reached their maximum possible extent, pastures make room for grasslands.

[43] These rules guarantee the priority for the establishment of pastures on former grasslands, even under conditions of back conversion of agricultural lands. Note that when converting agricultural lands back to natural vegetation, one has to account for the limited extent of natural vegetation in a grid cell. This maximum extent of natural vegetation is given by the distribution of potential natural vegetation (see section 3.6).

[44] Using the above conversion order, the extended land use transitions are derived as follows. Basic to this derivation are the (directed) conversion fractions

$$\Delta_{i\triangleright j} = T_{i\triangleright j} c_i, \quad i,j \in \{\{N|F,G\},C,P\}, \quad i \neq j, \tag{23}$$

that $i, j \in \{N,C,P\}$ are fully determined by the current vegetation distribution c_N, c_C, c_P, and the land use transitions between N, C, and P from the Harmonized Protocol. The aim is to determine the matrix elements for transitions from the natural vegetation types G and F to the agricultural types C and P, and vice versa all other matrix elements are known anyway (like $T_{C\triangleright P}$) or follow from them via equation (17).

[45] First the expansion of agricultural lands is considered, in particular (rule 1 and rule 2) the expansion of pastures. Formally, this expansion is characterized by $\Delta_{N\triangleright P} > 0$. The problem is to distribute the conversion fraction $\Delta_{N\triangleright P}$ to the separate conversion fractions from grasslands to pastures, and F-lands to pastures. We have

$$\Delta_{N\triangleright P} = \Delta_{G\triangleright P} + \Delta_{F\triangleright P}. \tag{24}$$

According to the sequential ordering of transitions described earlier, first, the transition G to P has to be considered, i.e., as much as possible of $\Delta_{N\triangleright P}$ has to be transferred to $\Delta_{G\triangleright P}$. Obviously, $\Delta_{G\triangleright P}$ can neither get larger than the currently available grasslands c_G, nor larger than the total amount $\Delta_{N\triangleright P}$ to be transferred. Hence,

$$\Delta_{G\triangleright P} = \min(c_G, \Delta_{N\triangleright P}), \tag{25}$$

so that using the definition (23) one finds the first of the desired matrix elements as

$$T_{G\triangleright P} = \min\left(1, \frac{\Delta_{N\triangleright P}}{c_G}\right) = \min\left(1, \frac{T_{N\triangleright P} c_N}{c_G}\right). \tag{26}$$

If insufficient grassland is available to allocate $\Delta_{N\triangleright P}$ fully, then, according to rule 2, for the remainder F-lands are used: from equations (24) and (25) one finds

$$\begin{aligned} T_{F\triangleright P} &= \min\left(1, \frac{\Delta_{N\triangleright P} - \Delta_{G\triangleright P}}{c_F}\right) \\ &= \min\left(1, \frac{T_{N\triangleright P} c_N - T_{G\triangleright P} c_G}{c_F}\right). \end{aligned} \tag{27}$$

[46] To handle rule 3 (i.e., the conversion of natural lands to croplands), one has to account for the grasslands and F-lands that according to rules 1 and 2 were already converted to pastures. These remaining cover fractions $\tilde{c}_G$ and $\tilde{c}_F$ of grasslands and F-lands are given as

$$\tilde{c}_G = (1 - T_{G \triangleright P}) c_G \tag{28}$$

$$\tilde{c}_F = (1 - T_{F \triangleright P}) c_F \tag{29}$$

so that the distribution of natural lands to crops can equally be written as

$$T_{N \triangleright C} c_N = T_{G \triangleright C} c_G + T_{F \triangleright C} c_F \tag{30}$$

or as

$$T_{N \triangleright C} c_N = \tilde{T}_{G \triangleright C} \tilde{c}_G + \tilde{T}_{F \triangleright C} \tilde{c}_F \tag{31}$$

where the newly introduced transition elements with a tilde describe the transitions with respect to the cover fractions already reduced by establishment of pastures. By rule 3 the establishment of crops happens at equal proportion with respect to these reduced cover fractions so that

$$\tilde{T}_{G \triangleright C} = \tilde{T}_{F \triangleright C} = \frac{T_{N \triangleright C} c_N}{\tilde{c}_G + \tilde{c}_F}, \tag{32}$$

where the last equality is a consequence of the first equality when using equation (31). Since the first and second right-hand terms in equations (30) and (31) must match separately one finally finds

$$T_{G \triangleright C} = T_{N \triangleright C} (1 - T_{G \triangleright P}) \frac{c_N}{c_N - \Delta_{G \triangleright P} - \Delta_{F \triangleright P}} \tag{33}$$

$$T_{F \triangleright C} = T_{N \triangleright C} (1 - T_{F \triangleright P}) \frac{c_N}{c_N - \Delta_{G \triangleright P} - \Delta_{F \triangleright P}}. \tag{34}$$

[47] Coming now to the shrinkage of agricultural lands, the respective rule 1 has to be considered first. Here $\Delta_{C \triangleright N} > 0$. Giving croplands back at equal proportion to the relative availability of grasslands and F-lands means that there is a common factor a for the transitions from croplands back to natural vegetation obeying

$$T_{C \triangleright G} c_C = a \left(c_G^{\text{pot}} - c_G \right) \tag{35}$$

$$T_{C \triangleright F} c_C = a \left(c_F^{\text{pot}} - c_F \right). \tag{36}$$

Here c_G^{pot} and c_F^{pot} are the potential (maximum) natural extent of grasslands and F-lands, respectively, in the sense of section 3.6. The factor a is limited in size because grasslands and F-lands cannot grow larger than their potential extent. A necessary condition for this is

$$T_{C \triangleright G} \leq \frac{c_G^{\text{pot}} - c_G}{c_C} \tag{37}$$

$$T_{C \triangleright F} \leq \frac{c_F^{\text{pot}} - c_F}{c_C}, \tag{38}$$

so that by comparison with equations (35) and (36)

$$a \leq \frac{1}{c_C}. \tag{39}$$

[48] On the other hand, using the obvious relation

$$T_{C \triangleright N} = T_{C \triangleright G} + T_{C \triangleright F} \tag{40}$$

together with (35) and (36), one can solve for a. Combining the resulting expression for a with condition (39) gives for the desired transition elements

$$T_{C \triangleright G} = \min \left(\frac{1}{c_C}, \frac{T_{C \triangleright N}}{c_N^{pot} - c_N} \right) \left(c_G^{\text{pot}} - c_G \right) \tag{41}$$

$$T_{C \triangleright F} = \min \left(\frac{1}{c_C}, \frac{T_{C \triangleright N}}{c_N^{pot} - c_N} \right) \left(c_F^{\text{pot}} - c_F \right). \tag{42}$$

[49] As a side remark it shall be noted that the conditions (37) and (38) would also be sufficient for assuring that grasslands and F-lands cannot grow larger than their potential extent if not at the same time also pastures could be given back to natural lands. Because this latter process is considered separately from back conversion of croplands, the approach developed here may in some rare cases lead to more grasslands or F-lands than potentially available. In the implemented algorithm this is checked at the end, and the problematic transitions are suppressed.

[50] Appling now rules 2 and 3 for the shrinkage of pastures it is straightforward to derive the following equations for the remaining two unknown matrix elements when noting $T_{P \triangleright N} = T_{P \triangleright F} + T_{P \triangleright G}$:

$$T_{P \triangleright F} = \min \left(T_{P \triangleright N}, \frac{c_F^{\text{pot}} - (c_F + T_{C \triangleright F} c_C)}{c_P} \right) \tag{43}$$

$$T_{P \triangleright G} = \min \left(T_{P \triangleright N} - T_{P \triangleright F}, \frac{c_G^{\text{pot}} - (c_G + T_{C \triangleright G} c_C)}{c_P} \right). \tag{44}$$

4.3. Daily Land Cover Transitions

[51] The discussion so far dealt with yearly land use transitions. But updating land cover only once a year may introduce shocks into the system. Therefore, the yearly land use transitions $T_{i \triangleright j}$ are interpolated to daily

land use transitions $T^{(d)}_{i\triangleright j}$, where d denotes the number of a day in a year.

[52] The idea is to interpolate the cover fractions linearly between the cover fractions c_i and c'_i of equation (20). Denoting the number of days in the current year by N_d this can be achieved by adding each day the same part

$$\delta_{i\triangleright j} = \frac{\Delta_{i\triangleright j}}{N_d}, \quad i \neq j, \tag{45}$$

of the conversion fractions (equation (23)). With equation (45) the daily cover fractions are given by

$$c_i^{(d)} = c_i + d \sum_{j\in\{F,P,G,C\}} \left(\delta_{j\triangleright i} - \delta_{i\triangleright j}\right), \quad i \in \{F,P,G,C\}. \tag{46}$$

Noting that $c_i^0 = c_i$ is the cover fraction of class i at the last time step of the previous year, and $c_i^{(N_d)} = c'_i$ the cover fraction at the last time step in the current year, this can be rewritten as

$$c_i^{(d)} = c_i + \frac{d}{N_d}\left(c'_i - c_i\right), \quad i \in \{F,G,P,C\}, \tag{47}$$

so that with these definitions the cover fractions increase or decrease linearly throughout the year. Daily land use transitions $T^{(d)}_{i\triangleright j}$ for day d can be defined in analogy to equation (23) by

$$\delta_{i\triangleright j} = T^{(d)}_{i\triangleright j} c_i^{(d)}, \quad i \neq j, \tag{48}$$

where $d < N_d$. By inserting equations (45), (47), and (23) the desired daily land use transitions are found as

$$T^{(d)}_{i\triangleright j} = T_{i\triangleright j}\frac{c_i}{N_d c_i^{(d)}} = \frac{T_{i\triangleright j} c_i}{N_d c_i + d\left(c'_i - c_i\right)}, \quad i \neq j. \tag{49}$$

With these definitions,

$$\begin{aligned}\sum_{j,j\neq i} T^{(d)}_{i\triangleright j} &= \frac{c_i}{N_d c_i^{(d)}} \sum_{j,j\neq i} T_{i\triangleright j} = \frac{c_i}{N_d c_i^{(d)}} \sum_{j,j\neq i} (1 - T_{i\triangleright i}) \\ &= \frac{c_i}{N_d c_i + d\left(c'_i - c_i\right)} (1 - T_{i\triangleright i}) \leq 1\end{aligned}$$

because both multiplicators in the latter expression are less or equal 1 for $d < N_d$. Hence,

$$0 \leq \sum_{j,j\neq i} T^{(d)}_{i\triangleright j} \leq 1 \tag{50}$$

so that by conservation of area (compare equation (17)) the diagonal term can safely be defined as

$$T^{(d)}_{i\triangleright i} = 1 - \sum_{j,j\neq i} T^{(d)}_{i\triangleright j}. \tag{51}$$

Thereby, the matrix relationship (18) also holds on daily basis:

$$\begin{aligned}c_i^{(d+1)} &= c_i^{(d)} + \sum_{j,j\neq i} \left(T^{(d)}_{j\triangleright i} c_j^{(d)} - T^{(d)}_{i\triangleright j} c_i^{(d)}\right) \\ &= c_i^{(d)} T^{(d)}_{i\triangleright i} + \sum_{j,j\neq i} T^{(d)}_{j\triangleright i} c_j^{(d)} \\ &= \sum_j T^{(d)}_{j\triangleright i} c_j^{(d)}, \quad i,j \in \{F,G,P,C\}.\end{aligned} \tag{52}$$

4.4. PFT Transitions

[53] In the previous sections it has been described how in JSBACH the (reduced) land use transitions of the Harmonized Protocol (equation (15)) are converted into the (extended) yearly transitions (equation (20)), and these finally into the daily transitions (equation (49)). The next task is to derive from the latter the PFT transitions (equation (18)). For brevity the superscript "(d)," indicating the dependence of the transition matrix on the particular day in the year, is dropped in the following.

[54] So far for the derivation of the (extended) transition matrix only the pasture rule has been used. For the derivation of the PFT transitions now the other two land distribution rules are invoked, i.e., the *pathway rule* and the *rule of equal relative gains and losses* (see earlier). On closer inspection, both rules are of similar structure: they demand that on land conversions (i) the relative loss of all PFTs in a shrinking land cover class is equal, and (ii) the relative gain of all PFTs in an expanding land cover class is also equal, although in the latter case "relative" means for the pathway rule relative to the current extent (c_i), whereas for the rule of equal gains and losses it means relative to the area currently available ($c_i^{\mathrm{pot}} - c_i$).

[55] To make this more precise, consider two land cover classes A and B from $\{F,G,P,C\}$. Each of these classes consists of a number of PFTs, which will be denoted by A_i and B_j, respectively, where the indices i and j number the PFTs in the particular class. Then, the two rules are expressed by

$$\frac{\Delta_{A_i\triangleright B}}{c_{A_i}} = \frac{\Delta_{A_j\triangleright B}}{c_{A_j}}, i \neq j, \text{"equal relative loss"} \tag{53}$$

$$\frac{\Delta_{A\triangleright B_i}}{x_{B_i}} = \frac{\Delta_{A\triangleright B_j}}{x_{B_j}}, i \neq j, \text{"equal relative gain"}, \tag{54}$$

where depending on the applied rule, x has the following meaning:

$$x_{B_i} = \begin{cases} c_{B_i} & \text{when applying rule 2} \\ c_{B_i}^{\mathrm{pot}} - c_{B_i} & \text{when applying rule 3,} \end{cases} \tag{55}$$

and $c_{B_i}^{\mathrm{pot}}$ is the maximally possible ("potential") cover fraction of PFT B_i. Here $\Delta_{A_i\triangleright B}$ is the fraction of the vegetated part of the grid cell that is transferred from

PFT A_i into the class of PFTs B. These rules are fulfilled when choosing the desired relationship between the elements of the (extended) transition matrix $\mathbf{T}$ and the matrix of PFT transitions $\mathbf{t}$ as

$$t_{A_i \triangleright B_j} = T_{A \triangleright B} \frac{x_{B_j}}{x_B}, \quad \forall A_i \in A, \forall B_j \in B. \tag{56}$$

That thereby equations (53) and (54) are indeed fulfilled is seen from

$$\frac{\Delta_{A_i \triangleright B}}{c_{A_i}} = \frac{\sum_{j=1}^{N_B} t_{A_i \triangleright B_j} c_{A_i}}{c_{A_i}} \overset{(56)}{=} \sum_{j=1}^{N_B} T_{A \triangleright B} \frac{x_{B_j}}{x_B} = T_{A \triangleright B}, \tag{57}$$

$$\frac{\Delta_{A \triangleright B_i}}{x_{B_i}} = \frac{\sum_{j=1}^{N_A} t_{A_j \triangleright B_i} c_{A_j}}{x_{B_i}} \overset{(56)}{=} \frac{T_{A \triangleright B}}{x_B} \frac{x_{B_i} \sum_{j=1}^{N_A} c_{A_j}}{x_{B_i}} = T_{A \triangleright B} \frac{c_A}{x_B}, \tag{58}$$

because the right-hand sides are independent of i (N_A, N_B denote the number of PFTs in the respective classes). Moreover, the following lines show that by equation (56) also the ratio between two shrinking PFTs as well as between two expanding PFTs is kept fixed, as was demanded in particular by the pathway rule:

$$\begin{aligned} \frac{c'_{B_i}}{c'_{B_j}} &= \frac{c_{B_i} + \Delta_{B_i \triangleright A} - \Delta_{A \triangleright B_i}}{c_{B_j} + \Delta_{B_j \triangleright A} - \Delta_{A \triangleright B_j}} \\ &= \frac{c_{B_i}}{c_{B_j}} \frac{1 + \frac{\Delta_{B_i \triangleright A}}{c_{B_i}} - \frac{\Delta_{A \triangleright B_i}}{c_{B_i}}}{1 + \frac{\Delta_{B_j \triangleright A}}{c_{B_j}} - \frac{\Delta_{A \triangleright B_j}}{c_{B_j}}} = \frac{c_{B_i}}{c_{B_j}} \end{aligned} \tag{59}$$

$$\begin{aligned} \frac{c'_{A_i}}{c'_{A_j}} &= \frac{c_{A_i} + \Delta_{B \triangleright A_i} - \Delta_{A_i \triangleright B}}{c_{A_j} + \Delta_{B \triangleright A_j} - \Delta_{A_j \triangleright B}} \\ &= \frac{c_{A_i}}{c_{A_j}} \frac{1 + \frac{\Delta_{B \triangleright A_i}}{c_{A_i}} - \frac{\Delta_{A_i \triangleright B}}{c_{A_i}}}{1 + \frac{\Delta_{B \triangleright A_j}}{c_{A_j}} - \frac{\Delta_{A_j \triangleright B}}{c_{A_j}}} = \frac{c_{A_i}}{c_{A_j}}; \end{aligned} \tag{60}$$

in these equations the last equality is obtained by using equations (57) and (58).

[56] Equation (56) gives the relation between land-class transitions $\mathbf{T}$ and PFT transitions $\mathbf{t}$ for all cases with enough space available for the expanding PFTs. But for back conversion of agricultural lands to natural vegetation it may happen that one or more natural PFTs cannot be expanded any more, because they reach their potential extent. In such a case, the transitions prescribed by the Harmonized Protocol turn out to be inconsistent with the distribution of natural vegetation in the model. This may happen for various reasons: one possibility is that during simulations after times of agricultural expansion, climate is changing such that the potential extent of natural vegetation shrinks to values smaller than at times when agricultural expansion started. This type of problem may also arise because the New Hampshire group has derived the transition matrices using their own distribution of natural vegetation that they derived from simulations of global biomass with the MIAMI model [*Hurtt et al.*, 2011]. A third possibility for the emergence of this problem may be related to the three land use distribution rules introduced here to implement the transitions: in some cases they may be too restrictive for the back conversion of agricultural land. The latter possibility could in principle be partly remedied, by distributing the surplus area to the other PFTs using once more the same formula (56), but for a smaller number of PFTs. But since this makes the algorithms even more complicated, and because it would affect under realistic scenarios only small areas on the globe, and finally because such an approach would not remedy a possible general inconsistency between the prescribed transitions and the natural vegetation in the model, a more simple strategy is used: we reduce the values of the transition matrix such that not more area of agricultural land is back-converted than available by potential natural vegetation. Therefore, for back conversions of agricultural lands equation (56) has to completed by the additional restriction

$$t_{A_i \triangleright B_j} c_{A_i} \leq c_{B_j}^{\text{pot}} - c_{B_j} \tag{61}$$

so that equation (56) then reads

$$t_{A_i \triangleright B_j} = \min\left(\frac{c_{B_j}^{\text{pot}} - c_{B_j}}{c_{A_i}}, T_{A \triangleright B} \frac{x_{B_j}}{x_B} \right), \quad \forall A_i \in A, \forall B_j \in B. \tag{62}$$

It should be noted that equation (61) is only a necessary, but not a sufficient condition, because it refers only to one of several parallel transitions increasing the area of PFT B_i. Therefore, after all transition elements have been computed, in a final check transitions that would impair the potential vegetation extent are suppressed.

[57] Finally, the diagonal elements of the transfer matrix follow from the conservation of area, namely, from an equation analogous to equation (17):

$$\sum_{j=1}^{K} t_{i \triangleright j} = 1, \quad i = 1, 2, \ldots, K, \tag{63}$$

which gives for the diagonal elements

$$t_{i \triangleright i} = 1 - \sum_{j=1, j \neq i}^{K} t_{i \triangleright j}, \quad i = 1, 2, \ldots, K. \tag{64}$$

4.5. Importance of the Pasture Rule

[58] Here we add some justification for the importance of the pasture rule that is integral part of our

model for anthropogenic land cover change. Using a biome mapping technique, *Strassmann et al*. [2008] find that almost 80% of the area converted to pastures since 1700 is claimed from natural lands without closed forest cover. Qualitatively, this is also supported by *Ramankutty et al*. [2006], who also mention regional exceptions: for example, the prairies in North America are largely converted to croplands, and conversely, large forest areas in Latin America are cleared for rangelands. But despite the first impression these are not counter examples to the validity of the pasture rule: the pasture rule affects only regions where alternatively forests or grasslands can be used, but this is not the case for the mentioned exceptions.

[59] To demonstrate the effect of the pasture rule, we now compare results from a simulation using the model as introduced earlier, with a simulation, where we replaced the pasture rule by a more simple approach: here pastures are allocated like crops at equal proportion on grasslands and F-lands (forests and shrublands; see section 7 for the model setup used in these simulations). It turns out that this makes a large difference for the global extent of forests: in the historical simulation using the pasture rule, forests decrease from 50.2 million km^2 in 1850 to 39.4 million km^2 in 2005. In the additional simulation with the more simple rule, forests decrease stronger, namely, down to 33.6 million km^2 in 2005. Particularly large is the effect of the pasture rule in savanna regions where the difference is up to 20% (see Figure 2), but except for the boreal zone (and deserts) where herding is rare, the effect is seen globally almost everywhere.

[60] It may be added that the validity of the pasture rule cannot be checked by comparing with literature estimates of global forest area. Different sources reveal 39.1 million km^2 for 2000 [*Strassmann et al*., 2008], 43.92 million km^2 for 1992 [*Ramankutty and Foley*, 1999], and 34.6 million km^2 for 1992 [*Pongratz et al*., 2008]. Obviously, the differences are similar to the effect from the pasture rule (5.8 million km^2, see above). This large variation is probably the result of uncertainties in the definition of the term "forest"; for example, the number by *Ramankutty and Foley* [1999] includes woodlands.

[61] Finally, it may be mentioned that in terms of carbon emissions from land use change, the effect of the pasture rule must be much larger than in terms of area: *Strassmann et al*. [2008] estimate that from the direct emissions arising since 1700 from the conversion to pastures those 20% of pastures that were established on forested areas contributed 70% due to the much larger biomass density of forests.

5. Natural Vegetation Cover Change in the Presence of Land Use

[62] In the last two sections it has been described how in JSBACH land cover changes are simulated separately for either natural vegetation dynamics (in the absence of land use) or anthropogenic land cover change (in the absence of natural vegetation dynamics). This section describes how to connect natural vegetation dynamics with anthropogenic land cover change.

[63] Such a component combining these two processes is necessary because concurrently with anthropogenic land cover change the composition of the natural vegetation may be altered by a climate change or other environmental factors (e.g., CO_2). For example, a forest may expand after pastures were introduced. How would farmers respond to the growing forest? One reaction could be to stay with the pastures at the same locations and cut down periodically all emerging trees. Another reaction could be to shift the pastures gradually to

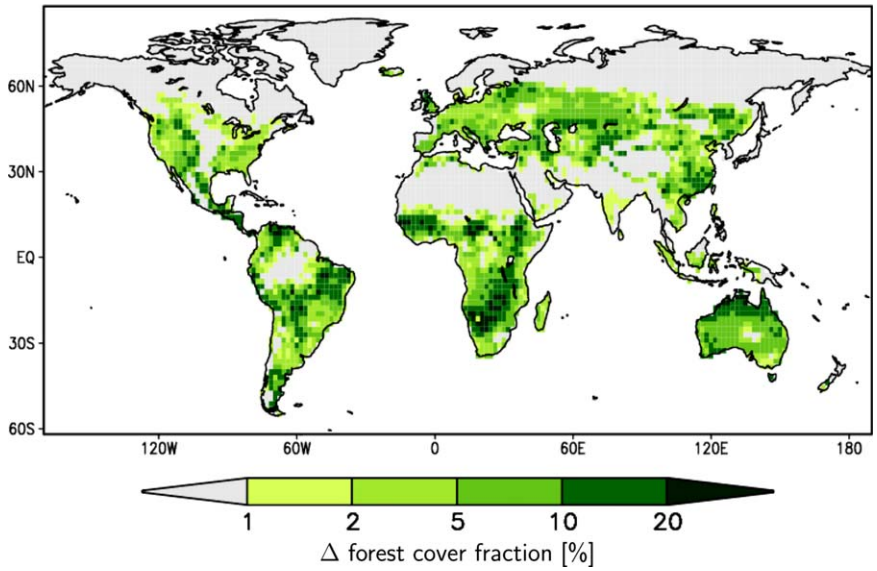

Figure 2. Additional forest cover due to the pasture rule as compared to a simulation where upon land use change pastures are allocated at former grasslands and forests at equal proportions. This figure is based on the results for the year 2005 as simulated by MPI-ESM-LR in experiment historical_r1i1p1-LR.

adjacent natural grasslands. Which option is chosen may depend on many socioeconomic factors like the existing infrastructure (location of settlements, and roads) and on the existing agrotechnology. But modeling such processes explicitly is beyond the scope of JSBACH, so that a more simple approach is needed.

[64] Obviously, such reactions of farmers to changes in the surrounding natural vegetation must be called anthropogenic land cover change. Therefore, the question arises whether such a type of land use change is already accounted for in the Harmonized Protocol. This protocol reflects two types of land use changes, namely, all changes affecting the net extent of croplands and pastures, and rotational land cover changes driven by certain agricultural practices like slash-and-burn. In contrast, the type of land use change in question concerns neither an expansion or shrinkage of agricultural activities, nor is it the result of a particular land use practice. Instead, it is a directed long-term adaptation of agriculture to changes in climate conditions by a very local translocation of croplands and pastures. Accordingly, we conclude that this additional type of anthropogenic land cover change is not included in the transitions described by the Harmonized Protocol and must therefore be represented independently in JSBACH.

[65] How could a simple representation of this additional land use change look like? The most direct approach would be to distribute pastures and croplands proportionally across the natural land cover types. But this would be completely inconsistent with the preferential establishment of pastures on grasslands ("pasture rule," see section 4.2). Alternatively one could distribute the known extent of pastures and croplands according to the pasture rule to the potential natural vegetation (instead of distributing it to the *remaining* natural vegetation as in the previous section). But this would lead to very large deviations from the vegetation distribution obtained by applying the pasture rule sequentially year by year during land use transitions because this sequential application introduces a dependence of the actual land cover on the full land use history that led to this land cover. This is illustrated in Figure 3: the upper graph shows a single land use transition from potential natural vegetation to cropland, which according to the rules set up in section 4.2 is established at equal proportion on grasslands and F-lands (i.e., forest and shrublands). In the lower graph the land use transition to cropland is done via an intermediate step where first F-lands are converted to pasture which in a second step is fully converted to croplands. In the first step the pasture rule has to be applied so that the pastures are fully established on grasslands. Although at the end in both graphs the extent of pastures and croplands is identical, the different land use histories give a different distribution for grasslands and F-lands. Hence, to describe land cover change due to changes in potential land cover, the actual state of land cover obtained during the historical development of land use cannot be ignored.

[66] The simple model described in the remainder of this section accounts for this. It is based on the following ideas. (i) Because of the socioeconomic aspects, the reaction of farmers to changing potential vegetation is conservative, allowing only small changes from year to year. (ii) On the other hand, since a land use adapted to the ruling climatic situation is advantageous for the farmers, one can assume that over several generations the land use distribution will be directed toward a distribution obtained from the pasture rule.

[67] Formally, the task is to translate the known distributions of potential vegetation given by equation (14) and the known land use as obtained by equation (18) into actual land cover c_i for all PFTs. To derive this land cover it is most convenient to consider first only the larger classes of vegetation F, G, C, and P (see section 4.1) before the land cover for all PFTs is derived.

[68] According to the above considerations, changes in climatic conditions and thus in potential vegetation lead to moderate shifts into the direction of a vegetation

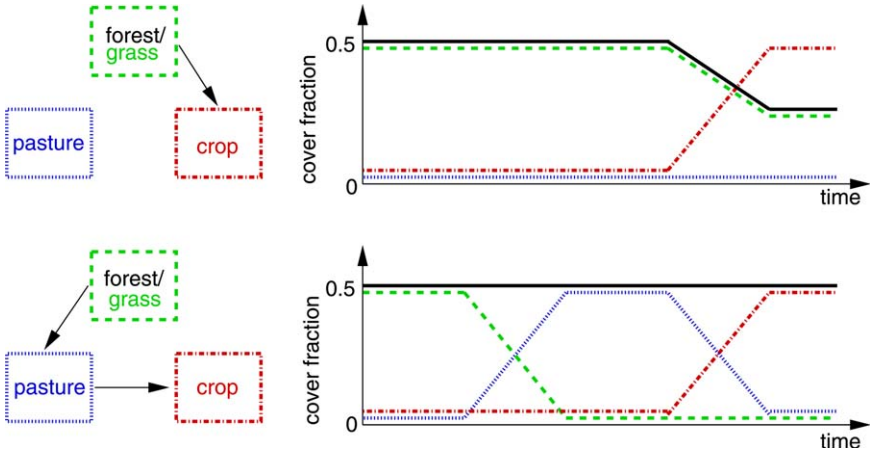

Figure 3. This graph illustrates that due to the pasture rule, cover fractions of the natural PFTs (forest, grass) depend on the history of land use transitions. The forest fraction is indicated by a solid black line; the grassland fraction is indicated by a dashed green line; the cropland fraction is indicated by a dashed-dotted red line; and the pasture fraction is indicated by a dotted blue line. For details see text.

distribution following the pasture rule. This "target cover fraction," called c^{inst} in the following, is obtained by assuming that the pasture rule is applied to the potential vegetation distribution as if all anthropogenic land cover change during history had happened *in one instant* by a single land use transition. Following the sequence of transitions for agricultural expansion described in 4.2 the first step in deriving these target fractions is to allocate pastures with priority on grasslands. Two cases have to be distinguished: in the first case there is enough grassland for the allocation of pastures ($c_P \le c_G^{\text{pot}}$), and in the second case also F-lands need to be converted to pastures. This gives

$$\left.\begin{aligned}\tilde{c}_G^{inst} &= c_G^{pot} - c_P \\ \tilde{c}_F^{inst} &= c_F^{pot}\end{aligned}\right\} \quad \text{for} \quad c_P \le c_G^{\text{pot}}$$
$$\left.\begin{aligned}\tilde{c}_G^{inst} &= 0 \\ \tilde{c}_F^{inst} &= c_F^{pot} - \left(c_P - c_G^{pot}\right)\end{aligned}\right\} \quad \text{otherwise} \tag{65}$$

From these intermediate values, indicated by a tilde over the symbols, in a second step the final target land cover fractions are obtained by distributing croplands proportionally to the remaining F-lands and grasslands. This gives for the F-lands

$$c_F^{inst} = \begin{cases} \tilde{c}_F^{inst} - c_C \dfrac{\tilde{c}_F^{inst}}{\tilde{c}_G^{inst} + \tilde{c}_F^{inst}} & \text{for} \quad c_P \le c_G^{\text{pot}} \\ \tilde{c}_F^{inst} - c_C & \text{otherwise} \end{cases}. \tag{66}$$

Using in accordance with equation (14) the relation $c_F^{\text{pot}} + c_G^{\text{pot}} = 1$, one obtains

$$c_F^{inst} = \begin{cases} (1 - c_P - c_C)\dfrac{c_F^{\text{pot}}}{1 - c_P} & \text{for} \quad c_P \le c_G^{\text{pot}} \\ 1 - c_P - c_C & \text{otherwise} \end{cases}. \tag{67}$$

The target cover fraction for grasslands c_G^{inst} follows from c_F^{inst} by noting that $c_F^{\text{inst}} + c_G^{\text{inst}} + c_P + c_C = 1$.

[69] Next the size of changes in land cover is determined that are induced solely by changes in potential vegetation. To this end a second, artificial target cover fraction for F-lands ${}^{-}c_F^{\text{inst}}$ is computed by entering into equation (67) *last year*'s potential vegetation but still using as for c_F^{inst} *this year*'s fractions of croplands and pastures c_P and c_C. The difference between these two target cover fractions $\delta_F^{\text{inst}} = c_F^{\text{inst}} - {}^{-}c_F^{\text{inst}}$ indicates how strongly natural land cover may have changed since last year at given land use. Changes arising from shifts in potential vegetation arise on top of the changes induced by land use. To derive the new land cover arising from both processes one thus needs in addition the cover fractions of natural vegetation that arose last year due to land use transitions alone; these cover fractions, denoted in the following by ${}^{-}c_i, i \in \{F, G\}$, result from the application of the Harmonized Protocol as described in the previous section. Assuming as discussed earlier that farmers follow changes in potential land cover only if it is advantageous for them, this year's new distribution of F-lands accounting for both processes can then be obtained by

$$c_F = \begin{cases} {}^{-}c_F + \delta_F^{\text{inst}} & \text{for mon}\left(c_F^{\text{inst}}, {}^{-}c_F^{\text{inst}}, {}^{-}c_F\right) \\ c_F^{\text{inst}} & \text{for mon}\left(c_F^{\text{inst}}, {}^{-}c_F, {}^{-}c_F^{\text{inst}}\right), \\ {}^{-}c_F & \text{for mon}\left({}^{-}c_F, c_F^{\text{inst}}, {}^{-}c_F^{\text{inst}}\right) \end{cases} \tag{68}$$

where $\text{mon}\,(a, b, c)$ means that a, b, and c are ordered monotonously, i.e., $a \le b \le c$ or $a \ge b \ge c$. The cases in equation (68) have the following meaning: in the first case ${}^{-}c_F$ is farther away from c_F^{inst} than ${}^{-}c_F^{\text{inst}}$ so that a correction by δ_F brings the cover fraction closer to the target c_F^{inst}. In the second case, an adjustment by the full size of δ_F would overshoot the target, so that the correction is made only until the target fraction is obtained. In the last case accounting for the correction, δ_F would drive the cover fraction away from the target so that the cover fraction is left unchanged from last to this year. The associated change in the fraction of grasslands can be obtained analogously, but it is simpler to compute it from the conservation of area by

$$c_G = 1 - c_F - c_C - c_P. \tag{69}$$

[70] Finally, after c_F and c_G have been determined, the new cover fractions of the natural PFTs are calculated by partitioning c_F and c_G into the different PFTs according to their relative abundance c_i^{pot}:

$$\begin{aligned} c_i &= c_i^{\text{pot}}\, c_F / c_F^{\text{pot}}, i \in \mathcal{W} \\ c_j &= c_j^{\text{pot}}\, c_G / c_G^{\text{pot}}, j \in \mathcal{G}. \end{aligned} \tag{70}$$

This simple scaling is justified by noting that the competition mechanisms implemented in DYNVEG operate on much smaller scales than the extent of the grid cells (10^4 km^2) so that the relative abundance of natural PFTs must considered to be rather uniform within a grid cell. Note that the expressions in equation (70) are evaluated only once a year, namely, during the first time step (compare Figure 4) so that the cover fractions c_G and c_F are those from the last time step of the year before.

[71] Overall, to account for climate-induced changes in natural vegetation the scheme for land cover change described earlier largely retains the unproportional translation of $c_F^{\text{pot}}, c_G^{\text{pot}}$ into c_F, c_G implied by the pasture rule but allows in addition for variations in c_F, c_G according to natural vegetation dynamics in the presence of managed land. Moreover, the scheme accounts for the history dependencies in c_F, c_G arising from the sequence of land use transitions but disperses them with time according to variations in the natural vegetation. In this way, c_F and c_G would converge on the long term to $c_F^{\text{inst}}, c_G^{\text{inst}}$, after land use transitions had ceased.

6. Sequence of Calculations

[72] Having presented in the previous sections the models for land cover change as implemented in JSBACH,

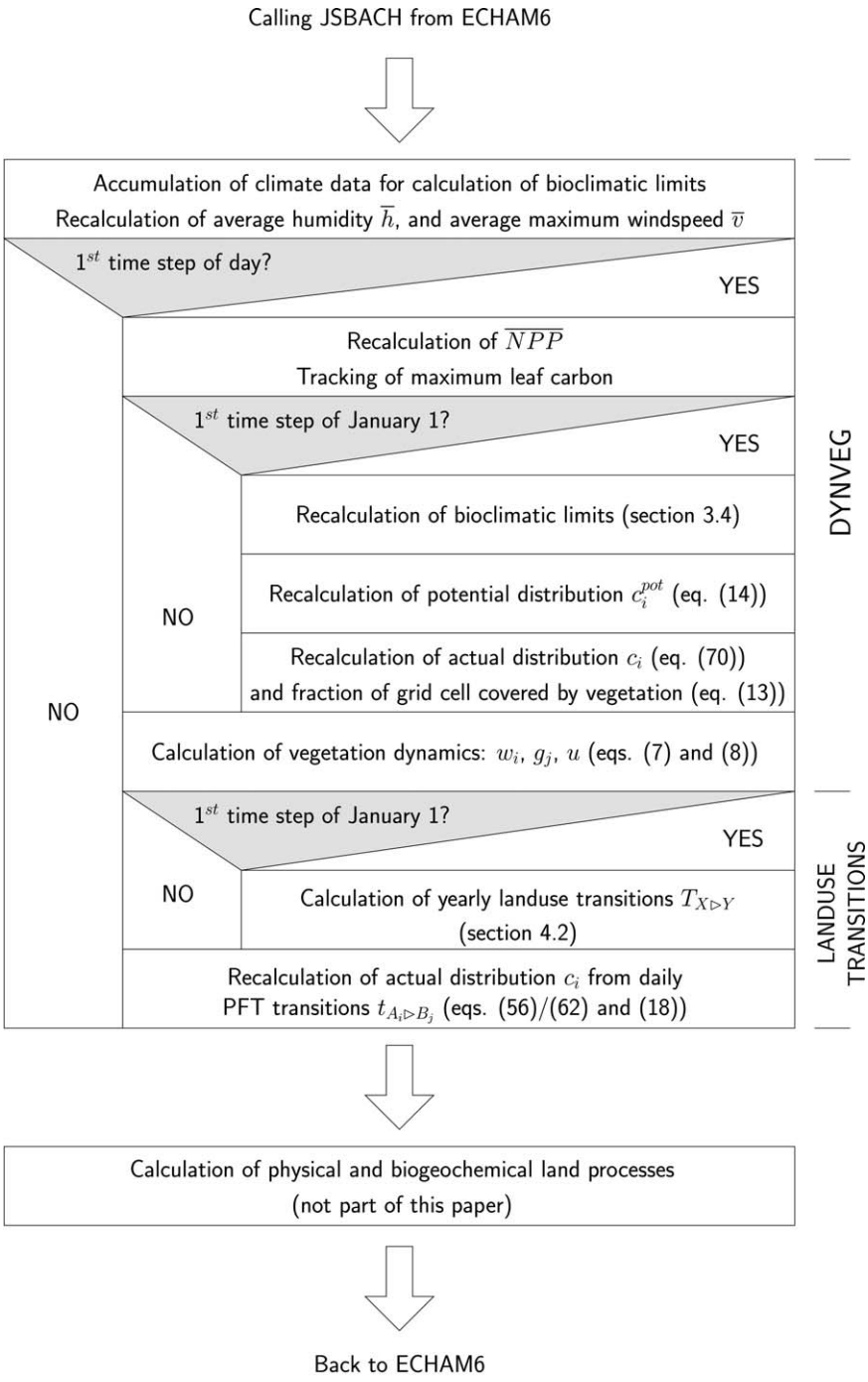

Figure 4. Sequence of calculations within one time step of JSBACH for the recalculation of land cover. The equation numbers refer only to the central equations that usually need various precalculations for their evaluation.

this section describes the sequential order in which the various model calculations are performed. The final result of this sequence of calculations is a daily update of the actual land cover fractions c_i for the different PFTs, as well as an annual update of $\text{veg}_{\max}$. These quantities are needed in the further calculations of JSBACH to compute all the physical and biogeochemical quantities that scale with the extent of the PFTs, like the exchange fluxes for heat, water, or CO_2 with the atmosphere.

[73] JSBACH is implemented as a subroutine of the atmospheric component ECHAM6 of MPI-ESM. Each model time step JSBACH is called once by ECHAM6. Within JSBACH, the calculation sequence starts with the model for natural land cover change (DYNVEG) followed by the model for anthropogenic land cover change before finally all other routines of JSBACH are called, involving all physical and biogeochemical land processes (compare Figure 4). The length of the time

step is prescribed from ECHAM6 driving JSBACH, which is typically of the order of 10 min but varies with model resolution.

[74] DYNVEG depends on several atmospheric quantities, provided by ECHAM6 when calling JSBACH. These quantities cannot be used directly but need to be smoothed in time. Hence, the calculation sequence begins with a recalculation of the time averages for relative air humidity $\overline{h}$ (see equation (10)) and maximum wind speed $\overline{v}$ (see equation (11)). This happens every time step. In contrast, bioclimatic limits (see section 3.4), involving also long-term averages, are recalculated only once a year. Nevertheless, each time step the necessary temperature information needs to be collected for later evaluation. In addition, DYNVEG depends on litter carbon for computing fire disturbances (see section 3.3), as well as a suitable time average $\overline{NPP}$ for the competition between PFTs (see equations (7) and (8)). Since carbon aspects are updated only daily within JSBACH, this recalculation of $\overline{NPP}$ is performed only every first time step of a day using the NPP that has been calculated by the biogeochemical parts of JSBACH for the previous day. For litter carbon, that is as well updated only once a day in JSBACH, a time average is not necessary. Similarly, information on biomass in leaves is tracked daily during a year to estimate maximum LAI for annual recalculation of $veg_{\max}$ (see equation (12)). Having performed the necessary precalculations, all information is available to update once a day the cover fractions w_i, g_i, and u_i via the central equations (7) and (8) of DYNVEG using an Euler discretization. The main results of DYNVEG are an update of the potential distribution of vegetation c_i^{pot} by equation (14) (needed for handling anthropogenic land cover change), an update of the actual vegetation distribution c_i with respect to natural land cover change in the presence of land use by equation (70), and an update of the fraction of a grid cell covered by vegetation $veg_{\max}$ from equation (13). These updates are performed only once a year during the first time step of 1 January.

[75] The Harmonized Protocol provides annual information for land use transitions between natural and agricultural lands. Every 1 January, this information is read in for the coming year and converted to the yearly land use transitions $T_{X \triangleright Y}$ (see section 4.2). Via equations (49) and (56)/(62) these are specialized each first time step of a day to the daily portion of the yearly transitions $t_{i \triangleright j}$ to be realized between the different PFTs; here c_i^{pot} determined by DYNVEG is used. Then, using $t_{i \triangleright j}$, the actual vegetation distribution c_i can be updated with respect to land use change by applying equation (18).

7. Discussion

[76] In the previous sections the models for natural and anthropogenic land cover change have been described as implemented in the land component JSBACH [*Raddatz et al.*, 2007] of MPI-ESM [*Giorgetta et al.*, 2013]. Results from simulations with the model for natural land cover change (DYNVEG) alone have already been presented earlier [*Brovkin et al.*, 2009]. In these simulations it became evident that in terms of tree cover convergence to a unique final tree cover distribution is obtained independent of its initial distribution so that in this respect the model exhibits no multistability. Since within the woody types the majority of land cover consists of forests, this result indicates that the competition between woody types and grasses even in interaction with climate has only a single stationary state. This implies nothing for the second, NPP-based competition mechanism within each of the two classes. But by analyzing analytically the fixed points of equations (7) and (8) and their stability, it can be rigorously shown (C. H. Reick et al., unpublished) that within each class under stationary conditions always the PFT with largest NPP is the only stable fixed point and thus will outcompete all other PFTs. Hence, we find no indication for multistability in this model. Accordingly, if mixtures of PFTs appear in a grid cell, they are the result of disturbances, which seems realistic on the level of broad vegetation groups (woody vs. grasses) like in savannas, but at the level of PFTs this is less clear: for example, mixed forests consisting of deciduous, evergreen, and coniferous trees may be stable even without disturbances because of climatically induced fluctuations in their bioclimatically allowed geographic range, or by small topographical differences in the terrain or in soil type [*Tang and Ohsawa*, 2002]: only the first of these aspects is part of our model, while at global scale the latter aspects are currently beyond our modeling capabilities.

[77] Compared to past CMIPs, in the recent CMIP5 not only climate forcing data are provided, but also consistent forcing data for land use change. The format of these latter data follows the New Hampshire Harmonized Land Use Protocol, which is technically based on the land use transition approach by *Hurtt et al.* [2006]. Upon full implementation of the Harmonized Protocol the climate modelers are in the position to perform scenario simulations highly consistent with the original computations performed by the scenario developers [*Hurtt et al.*, 2011]. In MPI-ESM we fully implemented the Harmonized Protocol with only two exceptions: first, the information on urban land use is ignored, and second the protocol distinguishes primary and secondary natural vegetation, which in our implementation have been lumped together to form a single class of natural vegetation (see section 4). This has been done because we so far have no model that could properly represent the difference between those two types of natural vegetation. Since secondary natural vegetation is characterized by past or ongoing human disturbances, one would need a model for forest management. There are indications that in terms of carbon sequestration primary forests are more efficient than secondary forests [*Luyssaert et al.*, 2008]. One can imagine that forest management also leads to biophysical differences between primary and secondary forests, e.g., in terms of albedo and evapotranspiration. Whether this is relevant in an Earth system context needs to be seen.

[78] An important pillar of our implementation of anthropogenic land cover change is the assumption that

pastures are preferentially established on former grasslands (''pasture rule''). This rule has been used earlier already in a study by *Houghton* [1999] to derive land use emissions and has also been employed by *Pongratz et al*. [2008] for a reconstruction of land cover maps for the last millennium. This rule introduces complications not only for implementing the land use transitions from the Harmonized Protocol (section 4.2) but also for combining the effects of natural and anthropogenic land cover change (section 5). In terms of forest cover the effect of the pasture rule is large (we simulate 15% less forest cover in 2005]. Data-based evidence on the validity of the pasture rule has been discussed in section 4.5. But this evidence refers to past agricultural expansion, whether this rule is also relevant for the future development of land cover, which is one field of application for ESMs, is less clear: with the further mechanization of agriculture [*Giedion*, 1987] and forestry [*Williams*, 2006], the effort necessary for deforestation and for the cultivation of deforested land decreases. Accordingly, in future this effort may not be any more an argument against deforestation to establish pastures. A similar question arises with respect to recultivation: the present implementation of anthropogenic land cover change assumes simply a reversal of the land distribution rules (see section 4.2), meaning in particular that forests are reestablished before natural grasslands. In view of several millennia of agricultural expansion, recultivation may play only a minor role for the study of past land cover change, except maybe regionally during periods of wars and epidemics [*Pongratz et al*., 2011] and also during early phases of recultivation [*Mather et al*., 1999]. But in the future the situation may be different: for example, the RCP4.5 scenario assumes an intense afforestation during the 21st century [*van Vuuren et al*., 2011a].

[79] As has been discussed in section 5, the pasture rule results in a dependence of land cover on the history of land use transitions (compare Figure 3). When applying the models for natural and anthropogenic land cover change simultaneously, the dynamics of natural vegetation must respect the anthropogenically modified distribution of natural vegetation types arising from land use change. Therefore, it is not per se clear how this can be achieved since the natural equilibrium between the different vegetation types is disturbed. One solution for this problem has been presented by *Strassmann et al*. [2008], who implemented land use change into the LPJ: since upon agricultural expansion they replaced natural vegetation cover at equal proportions by agricultural lands, the equilibrium between the different natural vegetation types was not disturbed. Accordingly, they could run the original LPJ dynamics for the natural vegetation cover that was designed for a world free of humans without any model changes. Since the evidence for the pasture rule indicates that the natural equilibrium of vegetation is disturbed by man, such an approach is questionable. As discussed in section 5, to account for such an anthropogenically induced disequilibrium in natural vegetation distribution, assumptions must be introduced on how agriculturalists react to changes in natural vegetation distribution. Our solution to the problem contains two elements. First, we allow the disequilibrium to change only by the size the potential vegetation cover (c^{pot}) changes. Second, we allow such changes only if they point into the direction of a hypothetical state (c^{inst}) where today's agricultural lands were allocated according to the land distribution rules (including the pasture rule!) in one instant out of a world without agriculture. In this way our model respects the historically developed disequilibrium. Since the changes in natural vegetation must be interpreted as a regional reallocation of agricultural areas, such changes represent human activities and it would be better to have more solid grounds for describing the reaction of agriculturalists to changes in natural vegetation. Especially when climate is changing fast, as assumed in ''business as usual'' climate scenarios, potential vegetation may undergo dramatic changes. In such cases this new type of anthropogenic land cover change that is not covered by the Harmonized Protocol (see the discussion in section 5) may not be ignorable. Further studies on this point seem necessary.

[80] The carbon cycle has been largely omitted in the present paper to keep this paper focused on land cover change. Nevertheless, in particular for the DYNVEG model, carbon aspects are important. They enter the model in several ways: both competition mechanisms depend directly (via NPP) or indirectly (via fire fuel in terms of litter) on plant productivity. In addition, our small submodel for the distribution of unhospitable land (see section 3.5) depends on the growth success of vegetation in the form of the maximum leaf area index. It is actually a large success that with this simple model the location of deserts can be determined rather realistically. In terms of albedo this is demonstrated in a companion paper by *Brovkin et al*. [2013] (compare also Figure 5). But carbon is also one of the major reasons for implementing the Harmonized Protocol: emissions from land use change cannot be measured directly but must be determined from model simulations. Accordingly, within JSBACH the model for anthropogenic land cover change has been fully embedded in its carbon cycle model. In particular also the harvest maps provided by the Harmonized Protocol can be used.

[81] Before concluding this paper, we show two results obtained with the models described in the present paper in simulations conducted as part of the recent CMIP5 simulations with MPI-ESM. This presentation of simulation results is only meant to illustrate certain aspects of the model dynamics, an evaluation of the resulting land cover in terms of tree cover and albedo is found in the already mentioned companion paper. How albedo is derived from land cover in JSBACH has been described by *Otto et al*. [2011].

[82] The simulation results shown later stem from simulations with the low-resolution version MPI-ESM-LR that consists besides JSBACH of the atmosphere model ECHAM6 (resolution T63 (1.9° × 1.9°), 47 levels reaching up to 0.01 hPa) [see *Stevens et al*., 2013], and the ocean model MPI-OM (resolution GR15 (approximately 1.6°), 40 levels) [see *Jungclaus et al*.,

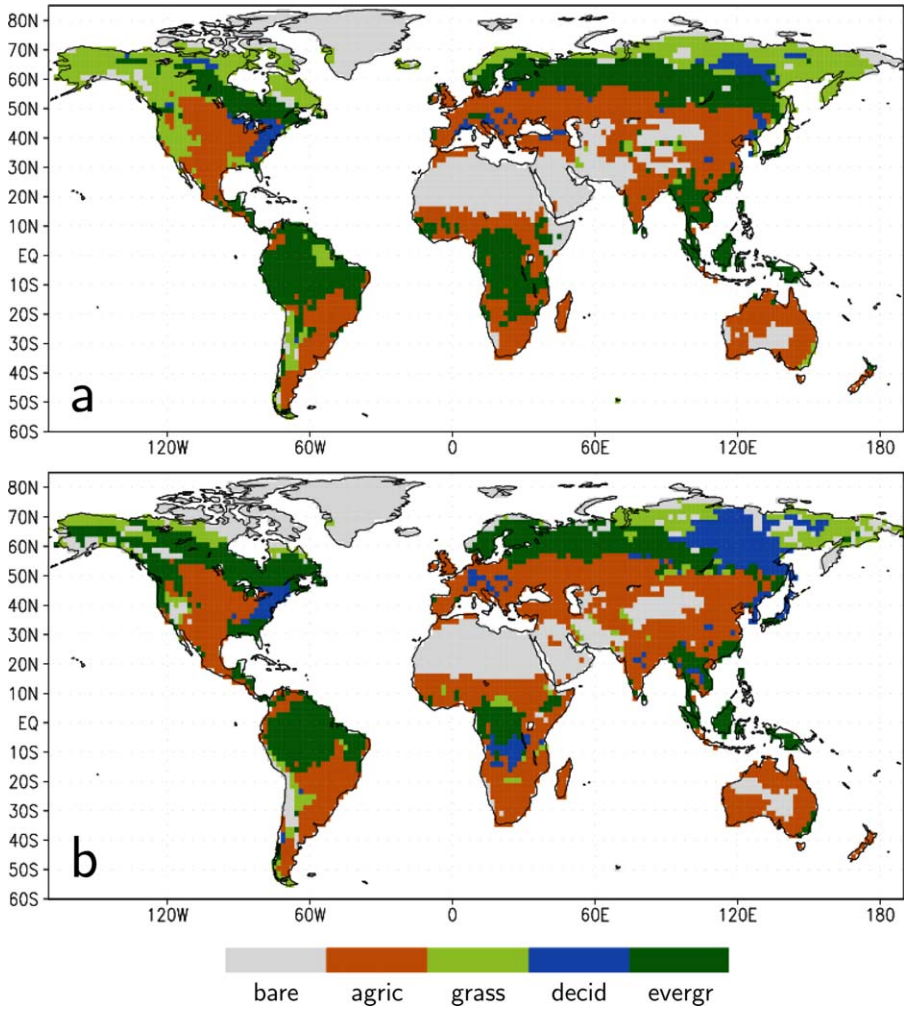

Figure 5. Dominant vegetation type for 2005 from (a) simulation with MPI-ESM-LR in experiment historical_-r1i1p1-LR and (b) a reconstruction of today's land cover following *Pongratz et al.* [2008] extended to 2005. Colors: gray: bare land; brown: agriculture (croplands and pastures); light green: grasslands; blue: deciduous forests; dark green: evergreen forests.

2006]. JSBACH is coupled to ECHAM6 via a subroutine call and is run on the same grid. In these simulations, 12 PFTs have been used, namely, those eight natural PFTs listed in Table 3, plus four agricultural PFTs for crops and pastures, each with a C3 and a C4 variant.

[83] Figure 5a shows the simulated distribution of the dominant land cover types at the end of our historical simulation [*Giorgetta et al.*, 2011a]. For comparison, Figure 5b shows the distribution of the same land cover types from the observation-based land cover reconstruction by *Pongratz et al.* [2008]. Overall, the resulting patterns match well, with some exceptions: in North America, particularly in Alaska, the evergreen forests do not extend sufficiently far to the west, and also the extent of deciduous forests in East Siberia is too small. It should be noted that the distribution of evergreen and deciduous forests is only partly determined by bioclimatic limits: the northern tree line arises for both types of forests from the same GDD criterion, and in Siberia the deciduous trees arise because it is too cold for evergreen trees (compare Table 4). In contrast, the appearance of deciduous forests in middle Europe and at the east cost of North America is a mere result of the NPP-based competition mechanism in DYNVEG (see the first right-hand term in equation (7)), since in these regions TC_{min} is irrelevant so that both types of forests, deciduous and evergreen, underlie identical bioclimatic limits.

[84] To illustrate the behavior of our model under a changing climate, we show in Figure 6 the results from simulations following the RCP2.6 scenario [*Giorgetta et al.*, 2011b]. The details of the scenario have been described by *van Vuuren et al.* [2011b]. The RCP2.6 scenario is particularly interesting because CO_2 peaks in the 21st century and declines thereafter (see inset in Figure 6b), as does the associated global temperature. The development of climate in this simulation is described by *Giorgetta et al.* [2013]. Figure 6a shows how the distribution of potential woody vegetation (compare

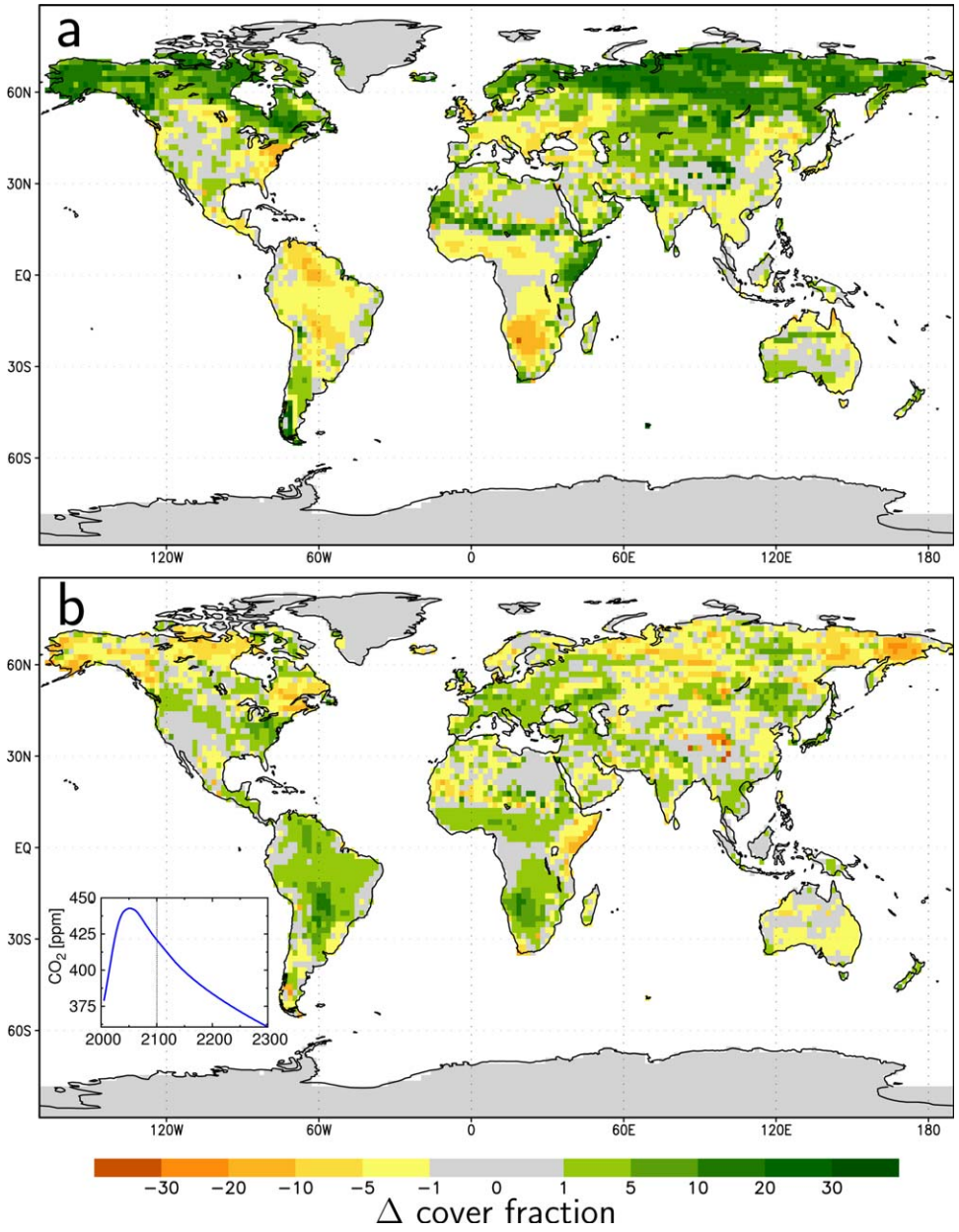

Figure 6. Change in potential land cover of woody vegetation types (forests and shrubs) in a simulation with MPI-ESM-LR for the scenario RCP2.6 (experiment rcp26_r1i1p1-LR). (a) Changes from 2005 to 2100 and (b) further changes from 2100 to 2300. The inset in (b) shows the development of the CO_2 concentration in this scenario.

equation (14)) changes from 2005 to 2100, and Figure 6b depicts the further change until 2300. As is well known from many scenario studies, upon rising CO_2 the boreal and subarctic regions experience a particularly large rise in temperature. This is consistent with the strong expansion of forests to the north during the 21st century (Figure 6a), leading to more than 30% increase in woody vegetation cover. In contrast, the dieback in the tropics, in particular of the Amazonian forests, is rather moderate (less than 10% cover loss), it is the consequence of decreasing precipitation in these regions. Upon the decline of CO_2 during the subsequent 200 years (Figure 6b) the tropical forests are recovering almost completely in this simulation, whereas the boreal expansion of forests is only partly reversed. In Amazonia the almost complete reversal can be explained by a recovery of precipitation to the level of 2005. Preliminary investigations show that the only incomplete reversal of the northward shift of boreal forests is related to an incomplete reversal of spring temperatures that are probably controlled by the behavior of the Arctic Ocean in this scenario, but this needs further investigation. Overall, in the combined system of land, atmosphere, and ocean processes the distribution of woody vegetation is at the considered time scales largely reversible in the tropics but not fully reversible at high northern latitudes.

[85] The distribution of vegetation and their changes shown in Figures 6a and 6b are the result of complex interactions among atmospheric, oceanic, and terrestrial processes. For the latter land cover and its changes play an important role, but only indirectly: the immediate effects arise from the exchange processes between land and atmosphere. But although they are physically identical everywhere, they are *quantitatively* different at different places on Earth. And this is where land cover comes into play: for example, due to albedo differences the radiative balance is different over grasslands and forests, going along with differences in evapotranspiration and energy fluxes as well as differences in land carbon uptake and release. From this point of view the concept of land cover classes is only a means to equip the various processes in models with geographically different parameter values and thereby helps to cope with the large heterogeneity in land cover. Unfortunately, there is no objective way for choosing land cover classes. Each choice remains a compromise because it may be necessary with respect to one process to distinguish different land cover types, although with respect to another process the role of this distinction may be largely unknown. Vegetation dynamics is one such case: the albedo difference between forests and grasslands is so large that it cannot be ignored in an ESM. Therefore in JSBACH, as the land component of an ESM, it necessarily needs separate classes for forests and grasslands. But on the other hand, the ecological knowledge necessary for a fully realistic treatment of the competitive dynamics of trees and grasses is rather incomplete. It would be desirable to understand the mechanisms that determine the time scales involved in biogeographic shifts. So far in DYNVEG the time constants have been chosen rather ad hoc on the basis of the lifetime of typical individuals, although such numbers are only partly relevant at the community level. Maybe paleo observations of vegetation shifts could be of help here. For such reasons, the DYNVEG model can only be one step on a longer road to a more knowledge-based dynamic biogeography model. With its description in the present paper we hope to have made its basic principles as well as its model details sufficiently transparent so that other researchers are able to point to insufficiencies and possible solutions. The same holds for our model of anthropogenic land use change. Using the pasture rule as a leading principle may not be uncontroversial.

[86] **Acknowledgment.** We thank Julia Pongratz for her numerous valuable comments and suggestions during manuscript preparation.

References

Begon, M., J. L. Harper, and C. R. Townsend (1999), *Ecology - Individuals, Populations, and Communities*, 3rd ed., Blackwell Sci., Oxford, U. K.

Bond, W. J. (2008), What limits trees in C_4 grasslands and savannas?, *Annu. Rev. Ecol. Evol. Syst.*, *39*, 641–659, doi:10.1146/annurev.ecolsys.39.110707.173411.

Brovkin, V., A. Ganopolski, M. Claussen, C. Kubatzki, and V. Petoukhov (1999), Modelling climate response to historical land cover change, *Global Ecol. Biogeogr.*, *8*, 509–517.

Brovkin, V., M. Claussen, E. Driesschaert, T. Fichefet, D. Kicklighter, M.-F. Loutre, H. D. Matthews, N. Ramankutty, M. Schaeffer, and A. Sokolov (2006), Biogeophysical effects of historical land cover changes simulated by six Earth system models of intermediate complexity, *Clim. Dyn.*, *26*, 587–600, doi:10.1007/s00382-005-0092-6.

Brovkin, V., T. Raddatz, C. H. Reick, M. Claussen, and V. Gayler (2009), Global biogeophysical interactions between forest and climate, *Geophys. Res. Lett.*, *36*, L07405, doi:10.1029/2009GL037543.

Brovkin, V., L. Boysen, T. Raddatz, V. Gayler, A. Loew, and M. Claussen (2013), Evaluation of vegetation cover and landsurface albedo in MPI-ESM CMIP5 simulations, *J. Adv. Model. Earth Syst.*, *5*, doi:10.1029/2012MS000169.

Catchpole, E. A., W. R. Catchpole, N. R. Viney, W. L. McCaw, and J. B. Marsden-Smedley (2001), Estimating fuel response time and predicting fuel moisture content from field data, *Int. J. Wildland Fire*, *10*, 215–222.

Chapin, F. S., J. T. Randerson, A. D. McGuire, J. A. Foley, and C. B. Field (2008), Changing feedbacks in the climate-biosphere system, *Front. Ecol. Environ.*, *6*, 313–320, doi:10.1890/080005.

Cheney, N. P., J. S. Gould, and W. R. Catchpole (1998), Prediction of fire spread in grasslands, *Int. J. Wildland Fire*, *8*, 1–13.

Claussen, M. (1997), Modeling biogeophysical feedback in the African and Indian Monsoon region, *Clim. Dyn.*, *13*, 247–257, doi:10.1007/s003820050164.

Claussen, M. (1998), On multiple solutions of the atmosphere-vegetation system in present-day climate, *Global Change Biol.*, *4*, 549–559.

Cox, P. M. (2001), Description of the TRIFFID dynamic global vegetation model, *Hadley Cent. Tech. Note* 24.

Cramer, W., et al. (2001), Global response of terrestrial ecosystem structure and function to CO_2 and climate change: Results from six dynamic global vegetation models, *Global Change Biol.*, *7*, 357–373.

Giedion, S. (1987), *Die Herrschaft der Mechanisierung*, Sonderausgabe, Athenäum, Frankfurt am Main, Germany. [originally published 1948 under the title *Mechanization Takes Command*, Oxford Univ. Press, U. K.]

Giorgetta, M. A., et al. (2011a), CMIP5 simulations of the Max Planck Institute for Meteorology (MPI-M) based on the MPI-ESM-LR model: The historical experiment, served by ESGF, *World Data Center for Climate*, CERA-DB "MXELhi." [Available at http://cera-www.dkrz.de/WDCC/CMIP5, doi:0.1594/WDCC/CMIP5.MXELhi.].

Giorgetta, M. A., et al. (2011b), CMIP5 simulations of the Max Planck Institute for Meteorology (MPI-M) based on the MPI-ESM-LR model: The rcp26 experiment, served by ESGF World Data Center for Climate, doi:10.1594/WDCC/CMIP5.MXELr2.

Giorgetta, M. A., et al. (2013), Climate and carbon cycle changes from 1850 to 2100 in MPI-ESM simulations for the Coupled Model Intercomparison Project phase 5, *J. Adv. Model. Earth Syst.* in press.

Goessling, H. F., and C. H. Reick (2011), What do moisture recycling estimates tell us? Exploring the extreme case of non-evaporating continents, *Hydrol. Earth Syst. Sci.*, *15*, 3217–3235, doi:10.5194/hess-15-3217-2011.

Harrison, S. P., I. C. Prentice, D. Barboni, K. E. Kohfeld, J. Ni, and J.-P. Sutra (2010), Ecophysiological and bioclimatic foundations for a global plant functional classification, *J. Veg. Sci.*, *21*, 300–317, doi:10.1111/j.1654-1103.2009.01144.x.

Houghton, R. A. (1999), The annual net flux of carbon to the atmosphere from changes in land use 1850–1990, *Tellus B*, *51*, 298–313.

Houghton, R. A. (2000), Interannual variability in the global carbon cycle, *J. Geophys. Res.*, *105*(D15), 20,121–20,130.

Hurtt, G. C., S. E. Frolking, M. G. Fearon, B. Moore, E. Shevliakova, S. Malyshev, S. W. Pacala, and R. A. Houghton (2006), The underpinnings of land-use history: three centuries of global gridded land-use transitions, wood harvest activity, and resulting secondary lands, *Global Change Biol.*, *12*, 1208–1229.

Hurtt, G. C., et al. (2011), Harmonization of land-use scenarios for the period 1500–2100: 600 years of global gridded annual land-use transitions, wood harvest, and resulting secondary lands, *Clim. Change*, *109*, 117–161, doi:10.1007/s10584-011-0153-2.

Jungclaus, J. H., N. Keenlyside, M. Botzet, H. Haak, J. J. Luo, M. Latif, J. Marotzke, U. Mikolajewicz, and E. Roeckner (2006), Ocean circulation and tropical variability in the coupled model ECHAM5/MPI-OM, *J. Clim.*, *19*, 3952–3972.

Jungclaus, J. H., et al. (2010), Climate and carbon-cycle variability over the last millennium, *Clim. Past*, *6*, 723–737, doi:10.5194/cp-6–723-2010.

Kabat, P., M. Claussen, P. A. Dirmeyer, J. H. C. Gash, L. Bravo de Guenni, M. Meybeck, R. Pielke, C. J. Vörösmarty, R. W. A. Hutjes, and S. Lütkemeier (Eds.) (2004), *Vegetation, Water, Humans and the Climate: A New Perspective on an Interactive System*, Springer, Berlin.

Kleidon, A., K. Fraedrich, and M. Heimann (2000), A green planet versus a desert world: Estimating the maximum effect of vegetation on the land surface climate, *Clim. Change*, *44*, 471–493.

Knorr, W. (2000), Annual and interannual CO_2 exchanges of the terrestrial biosphere: Process-based simulations and uncertainties, *Global Ecol. Biogeogr.*, *9*, 225–252.

Koeppen, W. (1900), Versuch einer Klassifikation der Klimate, vorzugsweise nach ihren Beziehungen zur Pflanzenwelt, *Geogr. Z.*, *6*, 593–611, and 657–679.

Koster, R. D., and M. J. Suarez (1992), A comparative analysis of two land surface heterogeneity representations, *J. Clim.*, *5*, 1379–1390.

Larcher, W. (1994), *Ökophysiologie der Pflanzen*, Ulmer, Stuttgart, Germany.

Lemmen, C., D. Gronenborn and K. W. Wirtz (2011), A simulation of the Neolithic transition in Western Eurasia. *J. Archaeol. Sci.*, *38*, 3459–3470.

Luyssaert, S., E.-D. Schulze, A. Börner, A. Knohl, D. Hessenmöller, B. E. Law, P. Ciais, and J. Grace (2008), Old-growth forests as global carbon sinks, *Nature*, *455*, 213–215, doi:10.1038/nature07276.

Mather, A. S., J. Fairbairn, and C. L. Needle (1999), The course and drivers of the forest transition: The case of France, *J. Rural Stud.*, *15*, 65–90.

McGuire, A. D., et al. (2001), Carbon balance of the terrestrial biosphere in the twentieth century: Analyses of CO_2, climate and land use effects with four process-based ecosystem models, *Global Biogeochem. Cycles*, *15*, 183–206.

Otto, J., T. Raddatz, and M. Claussen (2011), Strength of forest-albedo feedback in mid-Holocene climate simulations, *Clim. Past*, *7*, 1027–1039.

Pitman, A. J. (2003), The evolution of, and revolution in, land surface schemes designed for climate models, *Int. J. Climatol.*, *23*, 479–510.

Pitman, A. J., et al. (2009), Land use and climate via the LUCID intercomparison study: Implications for experimental design in AR5, *Geophys. Res. Lett.*, *36*, L14814, doi:10.1029/2009GL03907.

Pongratz, J., C. Reick, T. Raddatz, and M. Claussen (2008), A reconstruction of global agricultural areas and land cover for the last millennium, *Global Biogeochem. Cycles*, *22*, GB3018, doi:10.1029/2007GB003153.

Pongratz, J., C. H. Reick, T. Raddatz, and M. Claussen (2009), Effects of anthropogenic land cover change on the carbon cycle of the last millennium, *Global Biogeochem. Cycles*, *23*, GB4001, doi:10.1029/2009GB003488.

Pongratz, J., C. H. Reick, T. Raddatz, and M. Claussen (2010), Biogeophysical versus biogeochemical climate response to historical anthropogenic land cover change, *Geophys. Res. Lett.*, *37*, L08702, doi:10.1029/2010GL043010.

Pongratz, J., K. Caldeira, C. H. Reick, and M. Claussen (2011), Coupled climate carbon simulations indicate minor global effects of wars and epidemics on atmospheric CO_2 between AD 800 and 1850, *Holocene*, *21*, 843–851, doi:10.1177/0959683610386981.

Prentice, I. C., A. Bondeau, W. Cramer, S. P. Harrison, T. Hickler, W. Lucht, S. Sitch, B. Smith, and M. T. Sykes, (2007), Dynamic global vegetation modelling: Quantifying terrestrial ecosystem responses to large-scale environmental change, in *Terrestrial Ecosystems in a Changing World*, edited by J. Canadell, L. Pitelka, and D. Pataki, pp. 175–192, Springer, Berlin.

Quillet, A., C. Peng, and M. Garneau (2010), Toward dynamic global vegetation models for simulating vegetation-climate interactions and feedbacks: Recent developments, limitations, and future challenges, *Environ. Rev.*, *18*, 333–353, doi:10.1139/A10-016.

Raddatz, T. J., C. J. Reick, W. Knorr, J. Kattge, E. Roeckner, R. Schnur, K.-G. Schnitzler, P. Wetzel, and J. Jungclaus (2007), Will the tropical land biosphere dominate the climate-carbon cycle feedback during the twenty-first century?, *Clim. Dyn.*, *29*, 565–574, doi:10.1007/s00382-007-0247-8.

Ramankutty, N., and J. A. Foley (1999), Estimating historical changes in global land cover: Croplands from 1700 to 1992, *Global Biogeochem. Cycles*, *13*, 997–1027, doi:10.1029/1999GB900046.

Ramankutty, N., et al. (2006), Global land-cover change: Recent progress, remaining challenges, in *Land-Use and Land-Cover Change, Local processes and Global Impacts, The IGBP Series*, edited by E. F. Lambin and H. J. Geist, pp. 9–39, Springer, Berlin.

Sanderson, M. (1999), The classification of climates from Pythagoras to Koeppen, *Bull. Am. Meteorol. Soc.*, *80*, 669–673.

Sitch, S., et al. (2003), Evaluation of ecosystem dynamics, plant geography and terrestrial carbon cycling in the LPJ dynamic global vegetation model, *Global Change Biol.*, *9*, 161–185.

Sitch, S., et al. (2008), Evaluation of the terrestrial carbon cycle, future plant geography and climate-carbon cycle feedbacks using five dynamic global vegetation models (DGVMs), *Global Change Biol.*, *14*, 2015–2039, doi:10.1111/j.1365-2486.2008.01626.x.

Stevens, B., et al. (2013), The atmospheric component of the MPI-M Earth system model: ECHAM6, *J. Adv. Model. Earth Syst.*, doi:10.1002/jame.20015, in press.

Strassmann, K. M., F. Joos and G. Fischer (2008), Simulating effects of land use changes on carbon fluxes: Past contributions to atmospheric CO_2 increases and future commitments due to losses of terrestrial sink capacity, *Tellus B*, *60*, 583–603.

Sykes, M. T., I. C. Prentice, and W. Cramer (1996), A bioclimatic model for the potential distributions of North European tree species under present and future climates, *J. Biogeogr.*, *23*, 203–233.

Tang, C. Q., and M. Ohsawa (2002), Coexistence mechanisms of evergreen, deciduous and coniferous trees in a mid-montane mixed forest on Mt. Emei, Sichuan, China, *Plant Ecol.*, *161*, 215–230, doi:10.1023/A:1020395830795.

van Vuuren, D. P., et al. (2011a), The representative concentration pathways: An overview, *Clim. Change*, *109*, 5–31, doi:10.1007/s10584-011-0148-z.

van Vuuren, D. P., et al. (2011b), RCP2.6: Exploring the possibility to keep global mean temperature increase below 2°C, *Clim. Change*, *109*, 95–116, doi:10.1007/s10584-011-0152-3.

Westhoff, V., and E. van der Maarel (1973), The Braun-Blanquet approach, in *Ordination and Classification of Communities, Handbook of Vegetation Science*, vol. *5*, edited by R. H. Whittaker, pp. 617–726, Junk, Hague, Netherlands.

Williams, M. (2006), *Deforesting the Earth*, Univ. of Chicago Press, Chicago, Ill.

Corresponding author: C. H. Reick, Max Planck Institute for Meteorlogy, Bundesstr. 53, D-20146 Hamburg, Germany. (Christian.Reick@zmaw.de)